THE CRANFIELD INSTITUTE OF TECHNOLOGY

DEPARTMENT OF AERODYNAMICS

The Effect of Lift-system Airflow on the Hull Aerodynamics of Hovercraft

by

E.J. Andrews, B.Sc., C.Eng., F.R.Ae.S.

This report is the third and final report of a series of three reports on "External Aerodynamics of Hovercraft", Ministry of Technology Contract No. PD/28/033.

CONTENTS

ACKNOWLEDGEMENTS

The wind-tunnel model of the HD-2 research hovercraft was loaned to the Cranfield Institute of Technology by the Hovercraft Trials Unit of the Ministry of Technology.

Thank are due to the staff of the Aerodynamics Department of the Institute for their help in making modifications to the original model, in the development of compressed-air and vacuum systems for the laboratory, and in the preparation and conduct of the test programme.

Special thanks are due to Mr. J.R. Busing of the Department for his invaluable help with the automated data reduction programme.

SUMMARY

An attempt has been made to provide a better understanding of the influence of aerodynamic characteristics on the handling qualities of amphibious hovercraft.

This is the third and final report of a series of three reports in which the following have been explored.

(i) Aerodynamic characteristics of related hovercraft shapes;

(ii) the effect of cushion efflux on external aerodynamic characteristics, and finally;

(iii) the effects of lift-system airflow and the location of induction ports on the aerodynamic characteristics of hovercraft hulls.

It has been established that no major effects of consequence exist, yet at the same time, certain measures can be taken during the design stages of hulls, skirts and induction ports that will minimize inherent adverse characteristics.

The work was conducted under contract for the Ministry of Technology; Reference, Agreement No. PD/28/033/ADM, dated April 20th, 1967.

LIST OF SYMBOLS

A	intake area, $= 2 \times \pi d^2/4$	ft^2
d	port diameter	inches
d_t	strut-nozzle throat diameter	inches
h	hovergap	inches
l	reference (overall) length	feet
p_c	cushion pressure	lb/ft^2
q	dynamic pressure $= \frac{1}{2}\rho V^2$	lb/ft^2
Q_m	mass flow	slugs/sec
Q_v	volume flow	ft^3/sec
Q_w	weight flow	lb/sec
R	Reynolds number, $= Vl\rho/\mu$	
R_{subs}	balance weighbeam output	
S	reference area	ft^2
V	tunnel speed	ft/sec
V_i	intake velocity, $= Q_v/A$	ft/sec
β	angle of sideslip	degrees
ρ	density	$slugs/ft^3$
μ	viscosity	$lb.sec/ft^2$

Non-dimensional coefficients of -

C_h hovergap, = h/l

C_p cushion pressure, = p_c/q

C_{Q1} volume flow, = Q_v/SV

C_{Q2} or, = $Q_v/S\sqrt{2p_c/\rho}$

$C_{D,C,L}$ force along X, Y and Z wind axes = $\frac{\text{force lb}}{qS}$

$C_{l,m,n}$ moment about X, Y and Z wind axes = $\frac{\text{moment lb.ft}}{qSl}$

Test condition designators -

B model under influence of skirt efflux - blowing

G model under influence of gravitational effects

S model under influence of air induction - suction

W model under influence of tunnel wind

1. INTRODUCTION

A first generation of commercial amphibious hovercraft has now been operating on a scheduled basis with revenue payloads on relatively-short over-water routes. On some of these routes, open-sea conditions prevail. By and large, the degree of success attained during these operations has been encouraging. However, certain problem areas have been brought to light, one of the most important being concerned with handling qualities.

As in the case of aircraft, the handling qualities of hovercraft depend heavily on stability and control characteristics. In this case, however, the problem is rather more complex being dependent on aerodynamic, hydrodynamic, and air-cushion effects. There are also important interference effects at the aero-hydro-interface. To understand the overall handling problem, each of these contributory effects must be isolated from the others, so that individual study from a stability and control viewpoint can be attempted.

The task of isolation is difficult. It does not fall within the scope of full-scale testing, neither is it amenable to analysis except possibly in the case of air-cushion effects where good progress has been made using mathematical analysis. Thus it becomes essential that to study the aerodynamic and hydrodynamic effects, recourse be made to experimental testing. The National Physical Laboratory at Feltham has provided most of the effort in hydrodynamic experimentation, and the Cranfield Institute of Technology (formerly known as the College of Aeronautics) has complemented this work by undertaking the aerodynamic experimentation.

2. HANDLING QUALITIES OF AMPHIBIOUS HOVERCRAFT

Prerequisite to exploring the handling problem, it is necessary to examine the aerodynamic environment of the amphibious hovercraft. If the hovercraft be considered operating at a constant true speed in a wind which may have any bearing to the track of the hovercraft, then, dependent on the direction of that wind, the cruising airspeed of the hovercraft can vary substantially. At low true speeds, airspeeds may even be negative; and, operating yaw angles may be anywhere between $\pm 180^{\circ}$.

Longitudinal handling problems may be summarized as:

(i) the effect of wind direction on longitudinal trimming in cruise conditions;

(ii) trim changes due to sudden changes of power setting, and,

(iii) the plough-in and stern breakaway prelude to the catastrophic roll-over.

Low-speed lateral handling problems may be summarized as:

(i) the questionable value of fins which provide high-speed directional stability, and,

(ii) the problem of excessive drift in turning downwind.

High-speed lateral handling problems may be summarized as:

(i) the means by which centripetal force can be generated, and,

(ii) the avoidance of adverse yaw due to transverse asymmetric skirt contact/clearance at the aero-hydro-interface.

In reviewing these handling problems, it is concluded that close attention must be paid to the aerodynamic forces and moments along and about all three mutually perpendicular axes over a range of $\pm 180^{\circ}$ yaw, and over ranges of about $\pm 5^{\circ}$ of pitch and roll attitudes. Not until the complete aerodynamic picture is understood, can any parts of it be discarded as insignificant.

The aerodynamic characteristics of the hovercraft associate with the handling problems in the following manner:

Lift forces - plough-in, stern breakaway, and roll-over.

Drag forces - upwind and downwind performance, crosswind performance when $\beta \neq 0^{\circ}$, high-speed turning.

Pitching moments - cruise trimming, power-change trimming, plough-in and stern breakaway.

Crosswind forces - low-speed drifting and high-speed turning.

Yawing moments - low-speed directionable stability and high-speed turning.

Rolling moments - roll-over and high-speed turning.

Another full-scale problem, one not related to handling but nevertheless of aerodynamic origin and one significantly affecting performance, is that of momentum interference between the mutually perpendicular cushion-lift and air-propulsive systems.

In practice, it is manifest as a considerable loss in overall efficiency. In essence, it is due to undesirable mixing of the airflows of the two systems. It can be readily appreciated that the effect is very dependent on the relative location of the propulsive air-propellors and the lift-system air-intakes.

3. AERODYNAMIC TEST PROGRAMMES

In conjunction with national establishments and industry, it was decided that the aerodynamics of the hull of the hovercraft should be the first component of the configuration to receive attention. It was generally agreed that the aerodynamics of appendages such as fins, pylons, propellors, etc., already enjoyed a fairly comprehensive backlog of knowledge. Little was known, however, about the aerodynamics of a three-dimensional pseudo-aerodynamic shape having a large internal air-flow, one initially drawn from and finally mixing with a relatively-slow external air-flow.

The overall programme, planned to run several years, divided quite logically into three phases of progressive sophistication.

Phase I	Solid models affording a parametric study of the effect of hull shapes.
Phase II	Solid models with controlled air-cushion efflux.
Phase III	Hollow models with independently controlled air-induction and cushion-efflux systems.

Funded by the Ministry of Technology under Agreement PD/28/033/ADM, the programme of work has been completed at the Cranfield Institute of Technology, formerly known as the College of Aeronautics.

To provide a background to the Phase III programme of research reported herein, very brief descriptions of the two previous phases of research and a digest of the results obtained are set forth below.

Both previous phases of research have been reported upon in detail and separately.

3.1 PHASE I

Six-component wind-tunnel tests were performed at a Reynolds number of 0.77×10^6 on a family of related hovercraft shapes to determine aerodynamic characteristics. The models used in the tests were based on the shape of the HD-2 research hovercraft and were one foot long - 1/30th scale.

The work of this phase was fully reported in College of Aeronautics Memorandum No. 133, "The aerodynamic characteristics of a family of related hovercraft shapes ", E.J. Andrews, September 1967, (Ref. 1.).

The conclusions drawn from this parametric study are as follows:

(i) While the differing hull shapes certainly possess unique aerodynamic characteristics, there is a strong general similarity and most effects must be considered as second order.

(ii) Measured pitching and rolling moments were small and could not be considered of sufficient magnitude to make significant contributions to the overturning problem.

(iii) In spite of the above, a tenfold increase in lift, from headwind to beamwind conditions, could be a significant contributory factor.

(iv) Cruising performance and beamwind drifting are favourably affected by the use of large edge radii and sloping sides to the superstructure. Hull yawing moments are likewise minimized.

(v) The length of the foredeck does not appear to influence pitching moments to any significant degree. Other effects were as would be expected.

(vi) Inward tapered skirts have no particular merit over the full round type. In the case of the former, intense separation in the longitudinal V beneath the skirt was demonstrated. This accounts for the similarity in the drag levels of both types.

(vii) Inconsistent effects, ones not fully understood, involve the height of the superstructure. It is believed these effects may be due to the relative location of two edges each capable of generating individual separation. This might make an excellent topic for some basic research into separation effects behind bluff bodies.

3.2 PHASE II

The work performed in Phase II was published September 20th, 1968, as a College thesis by C.J. Richards - "The effect of cushion efflux on the external aerodynamics of a model hovercraft", (Ref. 2.).

One of the solid model configurations of Phase I was modified to include the capability of being tested in the wind tunnel with representative efflux from beneath the skirt of the model. These small model tests were followed by a similar series of tests on a larger model, a 1/12th scale model of the HD-2 hovercraft. The test Reynolds number for this larger model was 1.93×10^6. With both models, six-component wind-tunnel measurements and flow-visualixation tests were made.

The conclusions drawn from these tests are as follows:

(i) The effect of increasing cushion efflux on regions of separated flow around the skirt is to cause progressive flow reattachment. In turn, this reattachment causes a general flow clean-up and eliminates standing vortices.

(ii) The above effect is most pronounced near beam-wind conditions where a marked decrease in drag results. However, there is some increase in drag in head-wind conditions no doubt due to the cushion efflux acting as an effective increase in frontal area.

(iii) There is a tendency towards a reduction in cross-wind force with increasing cushion efflux. Large changes in crosswind force can be expected for beam-wind conditions.

(iv) Some increase in yawing moments is experienced with increasing cushion efflux.

(v) Other aerodynamic characteristics do not appear to be affected significantly by cushion efflux.

(vi) The boundary between free-stream and efflux air consists of a region of high vorticity.

4. EQUIPMENT - PHASE III

By comparison with the two previous phases of research, the Phase III tests involved the use of some quite sophisticated items of test equipment. These items required a special development programme and necessitated the construction of a special static test-rig. This was erected in the vicinity of the 8ft x 6ft wind tunnel and is shown in Figure 1.

The final result of the special development programme has been to provide the Institute with a unique hovercraft test facility - one capable of providing wind-tunnel tests on 3ft models at speeds up to about 150 feet per second in an 8ft x 6ft test section having a full-span groundboard and independently-controlled compressed air and vacuum systems. The latter system restricts the upper mass flow limit of the facility to about 1.5 pounds of air per second. The general arrangement of the facility is shown in Figure 2.

4.1 COMPRESSED AIR SYSTEM

To eliminate a source of mechanical constraint on the model, and hence on the wind-tunnel balance, the delivery of compressed air to the plenum chamber of the model was arranged as a rigid installation connected to the groundboard and the structure of the tunnel. There was no mechanical contact between this installation and the model.

High pressure air from the laboratory reservoir was fed through a measuring system external to the tunnel, and thence by two-inch bore piping into the tunnel terminating at a distributor located within the plenum chamber of the model. The rate of mass flow to the model was measured by a sharp-edged orifice plate. The orifice plate was calibrated in accordance with Reference 3, mercury manometers being used to establish the static pressure difference across the orifice plate and the static pressure in the piping upstream of the orifice.

A manually-operated sensitive reducing valve was used to regulate the mass flow for varying reservoir pressures and for appropriate clearances between the skirt of the model and the groundboard.

The terminal distributor is shown in Figure 3. It consisted of three annular flat plates of circular shape suitably blanked and baffled to give outward radial flow with a minimum of velocity components perpendicular to the plates. A reasonable uniformity of discharge around the circumference of the distributor was achieved by baffling with circumferentially disposed wire mesh.

The discharge was checked by observation of a water manometer connected to a hand-held pitot tube. In the final configuration, small variations in total head could only be detected in the vicinity of the entry of the compressed air to the distributor.

4.2 MODEL SUPPORT STRUT

The special model-support strut was designed as an integral part of the vacuum system. It consisted of a three-inch bore steel pipe connected to the main deck of the inverted model by a flush ring bolt. The strut was concentric with and passed through the compressed air distributor discussed above. A conventional mercury seal between the strut and the groundboard prevented the leakage of cushion pressure through the groundboard.

Intake air was drawn by the vacuum system into the model via the induction ports in its superstructure and thence into the bore of the support strut. In the support strut, an interchangeable standard convergent nozzle was provided. Two such nozzles were designed to choke at specific desired values of mass flow in accordance with design procedures outlined in R & M No. 3477, (Reference 4.). By such usage of a choked nozzle, regulation of the laboratory vacuum system was unnecessary. It was simply a case of fully opening a manually-controlled valve between the vacuum pumps and the model, and letting the choked nozzle restrict the flow to a desired value dependent on the selected nozzle in the support strut.

Prior to installation of the strut in the tunnel, nozzles were checked for mass-flow characteristics using the static test-rig. Measurements showed the nozzles to be performing within 2% of their design values.

The upper third of the model-support strut was structural in function only and was rigidly connected to the model-mounting platform of the balance. A crank in the top of the strut provided for the incorporation of a co-axial air connector between the laboratory vacuum system and the lower hollow portion of the support strut.

4.3 AIR CONNECTOR

The tests of Phase II had demonstrated very clearly that in the interests of balance sensitivity it was essential to adopt fairly elaborate measures to isolate the balance from all mechanical constraint. This had been achieved without difficulty in the case of the compressed air system planned for Phase III, but for the vacuum system the problem remained to be solved.

A solution to the problem was found in the use of the air connector shown in Figure 4. This connector is of a type developed and used satisfactorily by R.A.E., Bedford, and its use eliminates physical contact of the vacuum system with the balance. The principle of the air connector is illustrated in Reference 5. In this report, the applications of the connector relate to delivery of compressed air to models. In the current application involving a vacuum system, adherence to the basic principle is maintained, i.e., the leakage paths are convergent in the direction of high to low pressure.

In the air connector of Figure 4 a floating cap is provided between the terminal flange of the vacuum system and the hollow length of the model-support strut. The cap is isolated (i) from the vacuum system by inward radial leakage over the top of the cap, and (ii) from the support strut by upward axial leakage around the top circumference of the support strut. In operation, a small leakage of air, about 5% of the total flow, is permitted through the convergent leak paths so that the floating cap orients itself on surrounding air cushions. The weight of the floating cap is carried by low rate coil springs. The heavy side plates shown in Figure 4 are jigs used for assembly purposes only and are removed when installation is complete and tests are to be made.

Development tests in the static test-rig showed the cap to be orienting itself correctly on air cushions albeit with some vibration at frequencies considerably in excess of the natural frequency of the balance system. The oscillatory motion of the cap was such that at maximum amplitudes, point-contact friction forces between the cap and the support strut imposed angular momentum to the cap and caused it to rotate at about 10 seconds per revolution.

Tests were made with the model-support strut, including one of the two choked nozzles, and the air connector connected to the laboratory vacuum system. The model, the groundboard, and the compressed air system were not installed for these tests. Simulated aerodynamic loading was applied to the strut and balance readings confirmed that the operational vacuum system had negligible effect on force and moment measurements.

While in this configuration, calibration tests were made to obtain the effect on lift measurements of the low pressure in the upper portion of the strut above the choked nozzle. Calibrations were obtained for both nozzles.

4.4 MODIFIED HD-2 MODEL

The HD-2 model used in the Phase II tests had a solid superstructure. For Phase III it was necessary to construct a new hollow superstructure having the same external lines as the original solid model. The new superstructure was of mahogany construction with wall thicknesses of about one-half inch.

The new superstructure is shown in Figure 5. It incorporated nine alternate pairs of induction ports. Each pair was symmetrically disposed about the plane of symmetry of the model in the following locations.

Port-pair Locations	Model Config. No.
Rearward-facing windshield (HD-2 position)	1
Superstructure sidewall - aft	2
roof - aft	3
sidewall - mid	4
roof - mid	5
sidewall - forward	6
roof - forward	7
Forward-facing windshield**	8
Superstructure roof - one forward, one aft	9

4.5 WIND TUNNEL

Tests were conducted in the 8ft x 6ft low-speed wind tunnel located in the laboratory of the Department of Aerodynamics at the Cranfield Institute of Technology. This wind tunnel is of continuous return-flow type and operates at atmospheric pressure. It has a maximum speed capability of 250 feet per second corresponding to $R_e = 1.6 \times 10^6$ per foot.

The tunnel is equipped with a six-component overhead Warden-type virtual-centre balance having four remotely-operated weigh-beams referenced to a wind-axis system. Two modes of operation, with a remotely-controlled mechanical changeover, are provided. The first mode provides direct measurement of lift and drag forces and yawing moment, with indirect measurement of crosswind force. The second mode provides direct measurement of pitching and yawing moments and indirect measurement of rolling moments. The sign convention of the forces and moments of the balance system, as obtained from Reference 6, are shown in Figure 7.

** Because of insufficient windshield depth, these ports were elliptical in shape. However, their intake area was the same as all other ports which were circular in shape. Figure 6 gives full details of port dimensions and locations.

Balance outputs are available on dials and on eight-hole punched tape. During the tests subsequently described, both methods were employed the latter being used in conjunction with a Fortran programme for automatic data reduction.

The groundboard of the tunnel is of wooden construction eight feet square and two inches thick. It has an elliptical leading edge and a chamfered trailing edge and is adjustable to zero incidence relative to the tunnel flow by means of turn-buckles.

A metal fairing between the groundboard and the tunnel roof housed all necessary piping for the compressed-air system and the model-support strut which incorporated elements of the vacuum system.

A pitot-static head mounted on the floor of the tunnel about 20 inches beneath the inverted model was used with a Betz manometer to maintain constant speed in the test section. This was necessary because of varying blockage effects as the model was rotated through the yaw range.

The wind-tunnel installation is shown in Figure 8.

5. PROGRAMME OF TESTS - PHASE III

Utilization of test facilities in conducting the necessary programme of tests was as follows.

5.1 STATIC TEST FACILITY

Period - November 10th to 28th, 1969.

(i) Development tests of compressed-air distributor.

(ii) Measurements of mass flow through choked nozzles.

(iii) Development tests of air connector.

(iv) Assembly checking with support strut, groundboard, mercury seal, compressed-air distributor, and model.

5.1.2 WIND TUNNEL TEST FACILITY

Period - December 5th, 1969 to January 6th, 1970.

(i) Confirmation of balance accuracy.

(ii) Support strut calibrations.

(iii) Preliminary check runs.

9 days rigging
2 days idle due to sickness
6 days testing (27 hours tunnel time)
Total 17 working days

Period - February 24th to March 5th, 1970.

Measurement runs

3 days rigging
1 day fault-finding
4 days testing (10 hours tunnel time)
Total 8 working days

Period - August 4th to September 17th, 1970

Measurement runs

4 days rigging
2 days fault-finding
4 days idle due to programme interference
22 days testing (80 hours tunnel time)
Total 32 working days

5.2 WIND TUNNEL TEST DATA

5.2.1 TUNNEL OPERATING CONDITIONS

Speed, V	= 120 ft/sec
Reynolds number, R	= 1.93×10^6
Dynamic pressure, q	= 17.1 lb/ft^2
	= 83.7 mm water

5.2.2 MODEL DATA

Configurations (Para. 4.4)	1 to 9 inclusive
Attitude - pitch	0°
roll	0°
yaw	0° to 180°
Port diameter, d	= 2.25 inches
Intake area, A	= 2 x 0.0276 ft^2
Reference area, S	= 2.98 ft^2
Reference (overall) length	= 2.5 ft
Centre of gravity position	Mid-beam, mid-length $3\frac{1}{4}$ inches below groundboard
Hovergap, h	= 0.10 inches
Hovergap coefficient, C_h	= 0.0033

5.2.3 LIFT SYSTEM AIRFLOW

Strut-nozzle throat diameter, d_t	= 1.09	= 1.475 inches
Weight flow, Q_W	= 0.55	= 1.00 lb/sec
Mass flow, Q_m	= 0.0171	= 0.0311 slugs/sec
Volume flow, Q_v	= 7.20	= 13.1 ft^3/sec

Volume flow coefficient, C_{Q1}	= 0.0201	= 0.0365
or, C_{Q2}	= 0.0238	= 0.0241
Cushion pressure, p_c	= 12.2	= 39.0 lb/ft^2
Cushion pressure coefficient, C_p	= 0.715	= 2.28
Intake velocity, V_i	= 130	= 237 ft/sec

5.2.4 BALANCE RECORDINGS

For all tests, balance recordings of the following were taken

Mode 1 (forces) R_1 R_2 R_3 R_4

Mode 2 (moments) R_{2A} R_{3A} R_{4A}

The relationship of this balance data to conventional force and moment data has been discussed in Para. 4.5 and is illustrated in Figure 7.

For all model configurations and at each test angle of yaw, the foregoing were obtained for the model when under the influence of the following.

Gravitational effects	G
Tunnel-wind effects,	W
Skirt-efflux (blowing) effects,	B
Air-induction (suction) effects,	S

Initially, test combinations of the foregoing effects were as follows.

G, GWBS, GWB, GWS, GBS, GB, GS and GW

In later stages of the test programme, the above were reduced to

G, GWBS, GWB, GWS and GBS

5.3 PRESENTATION OF RESULTS

All tests were conducted at a tunnel speed of 120 ± 0.25 ft/sec corresponding to a test Reynolds number of 1.93 x 10^6. The full-scale Reynolds number of the HD-2 hovercraft at a cruising speed of 40 knots is 13.0 x 10^6.

All results have been obtained from a computerized data reduction programme and refer to the wind-axis system of the balance. This axis system is shown in Figure 7 and it should be noted that it differs from the more commonly used "stability axes".

With this wind-axis presentation, a drag force at 90^o angle of sideslip corresponds to a lateral force referenced to body axes. Additionally, at this angle of sideslip, a crosswind force in wind axes corresponds to a longitudinal force in body axes. Similarly, at 90^o angle of sideslip, a pitching moment corresponds to a rolling moment about the longitudinal axis of the model, and vice versa.

All results are presented in the form of conventional non-dimensional coefficients as previously defined.

6. DISCUSSION OF RESULTS - PHASE III

6.1 AERODYNAMIC CHARACTERISTICS OF HD-2 MODEL

The aerodynamic characteristics of the basic HD-2 model, designated Configuration 1, are shown in Figures 9 through 15.

During the course of the test programme, all data for the no-flow condition of this configuration was measured twice. It will be seen from the plotted data that repeatable characteristics were measured. For lift forces this is quite remarkable since maximum measured lift forces were less than 2% of the lift balance capability.

However, in conditions of simulated airflow through the model, both lift and drag data exhibited lack of accuracy and repeatability. Tests performed with cushion efflux only, as described in Reference 2, experienced the same problems. Since calibration tests performed on the strut alone produced steady repeatable results, it must be concluded the abnormalities during the tunnel test programme are of aerodynamic origin. It is recommended therefore that lift and drag data in particular be considered open to question on account of limitations in technique.

The measured lift data shown in Figure 9 is meaningless unless corrected for two effects. The first of these is that a negative lift force is measured by the balance in conditions of induction due to the low pressures in the upper portion of the strut above the choked nozzle. This negative lift is dependent on the mass flow, and hence it varies with the diameter of the throat of the choked nozzle. As mentioned previously, corrections were easily obtained by calibration with the model removed from the strut.

The second effect that must be corrected is that due to the lift generated by cushion pressure. Method B of Reference 2 was used to obtain these corrections.

Applying the foregoing corrections gives the lift data shown in Figure 10. It will be seen that within the limitations of accuracy discussed above, at low flow there is no effect from combined efflux and induction, whereas at high flow there is a marked loss of lift. It will be shown later that the loss of lift due to blowing is greater than the increase in lift due to suction.

Drag data is shown in Figure 11. For no-flow conditions, the data is well-defined and repeatable - for flow conditions, accuracy is somewhat questionable. It is immediately apparent, however, that the combined effects of cushion-efflux and air-induction are far more complex than the single effect of cushion-efflux. Throughout the sideslip range, the following effects might be expected in varying degrees.

(i) Air-induction would tend to suppress separation and hence reduce drag. It would cause an increase in momentum drag in headwind conditions and a decrease in tailwind conditions.

(ii) Cushion efflux is known to clean-up the flow around the skirt in beamwind conditions and to cause an increase in form drag in headwind and tailwind conditions.

It it quite evident from the data that follows that air-induction has a significant effect on the aerodynamic characteristics discussed subsequently. It is not unreasonable, therefore, to assert that dependent on the aspect that the induction ports present to the relative wind, separations from varying sources are modified, or suppressed, with the total effect on drag as shown in Figure 11. Detailed explanations can only be offered after further testing in greater detail with improved accuracy.

The following data on pitching moment, yawing moment, crosswind force and rolling moment are quite different from those measured in Reference 2. Since subsequently discussed results indicate that suction effects do not account for these differences, it is believed that there has been a general improvement in balance sensitivity due to the new plenum distributor and the air connector of the vacuum system.

Pitching moment characteristics are shown in Figure 12. It will be seen that in headwind conditions, increasing mass flow causes a nose-down pitching moment contribution, and that in tailwind conditions the contribution is in the tail-up sense.

Yawing moments are shown in Figure 13. Unstable moments are shown to increase substantially with increasing mass flow in both head and tailwind conditions.

Crosswind force data is shown in Figure 14. Mass flow substantially reduces the crosswind force when the relative wind is on the forward quarter; but when the relative wind is on the rear quarter, crosswind forces substantially increase with mass flow.

Rolling moment data for the HD-2 configuration is shown in Figure 15. The no-flow characteristics are primarily due to lift forces generated under the bow of the craft. The effect of mass flow is to markedly increase the negative, lee-down, rolling moment throughout the sideslip range. (In comparing this data with that of Reference 2, it should be noted that in Reference 2 there are inconsistencies of signs, although not of sense.)

6.2 EFFECTS OF LOCATION OF INDUCTION PORTS AT C_{Q1}=0.0365

The effects of the differing locations of the induction ports of Configurations 1 through 9 are shown in Figures 16 through 21. The data presented relates to the high mass flow condition with C_{Q1} = 0.0365.

The characteristics of Configurations 2 through 9 are shown in the form of coefficient increments from the base values of those coefficients for Configuration 1. Offset plotting of results has been used and thus, if the characteristics of Configurations 2 through 9 showed no change from those of Configuration 1, a series of equally spaced parallels would result.

For reasons discussed previously, the lift data of Figure 16 must be considered to be of questionable accuracy. Nevertheless, there is some indication of a trend to increasing lift coefficient when induction ports are located in the forward half of the superstructure. The trend is more clearly seen from the summarized lift data shown in Figure 42.

The drag increments shown in Figure 17 indicate that the drag characteristics of Configuration 1 differ from the drag characteristics of the other configurations. At sideslip angles up to about 70°, the other configurations show a larger increase in drag than does Configuration 1. It is conceivable that being located in the corners of the rear windshield the induction ports of this configuration are suppressing separation from the vertical edges of this windshield. The spread of the drag changes for Configurations 2 through 9 are shown in Figure 42. It will be seen that the drag increases in the 0° to 70° range of sideslip angles are greater than the drag decreases in the 80° to 180° range.

Changes in pitching moment characteristics are shown in Figure 18. Location of induction ports is shown to have little effect apart from a trend to increased nose-up pitching moment as induction ports move forward on the superstructure.

The yawing moment data of Figure 19 shows that Configurations 2 through 9 possess more unstable characteristics than does Configuration 1. This is possibly due to the suppression of the separation mentioned in the discussion of the drag changes. It will be noted that the data for Configuration 8 is more identifiable with that for the Configuration 2 through 9 group than with that for Configuration 1. It is suggested that this might be due to foredeck interference in the case of Configuration 8 and that with this configuration the slant of the vertical edges of the forward windshield is appreciably greater than that of the vertical edges of the rear windshield of Configuration 1. Less separation would originate from the more slanted edges.

Increments in crosswind force are shown in Figure 20. By comparison with Configuration 1, it will be seen that Configurations 2 through 9 exhibit increased positive force throughout the sideslip range. The effect is greatest at about 50° angle of sideslip. The common trend for Configurations 2 through 9 is attributable to separation changes originating from the vertical edges of the rear windshield.

The rolling moment data of Figure 21 indicates lee-up increases in the 0° to 90° range of sideslip angles and lee-down increases in the 90° to 180° range. With rear induction ports the lee-up effect is greater than the lee-down effect, but with forward ports the lee-up effect is less than the lee-down effect.

6.3 COMPARATIVE EFFECTS OF WIND, BLOWING AND SUCTION

6.3.1 INDIVIDUAL EFFECTS OF TUNNEL WIND

The effects of tunnel wind have been obtained for each of the nine configurations by obtaining the difference between characteristics measured in conditions of GWBS and GBS, when $C_{Q1} = 0.0365$.

Lift data is shown in the offset plotting of Figure 22. Since strut suction effects are the same in both test conditions, corrections are unnecessary. However, in Reference 2 it was established that tunnel wind had the effect of decreasing cushion pressure. Consequently, the cushion pressures of condition GBS would be greater than for condition GWSB. Assuming all configurations to be thus affected equally, no cushion pressure corrections have been included in the data of Figure 22. However, in the summarized data of Figure 40, such corrections have been included. The general effect of wind, as might be expected, is that all configurations are similarly affected.

The drag increments due to wind are shown in Figure 23. As has been mentioned previously, Configuration 1 appears to experience smaller drag increases in the 0° to 70° range of sideslip angles than do the other configurations.

Pitching moment increments are shown in Figure 24. All configurations appear to be affected equally.

From Figure 25 there appear to be no significant differences between configurations due to the effects of wind. All configurations show destabilizing effects due to wind.

Crosswind force increments due to wind are shown in Figure 26. All configurations show similar tendencies and while differences do exist they are but of minor nature.

The increments of rolling moment due to wind are shown in Figure 27. All configurations show the same tendencies - lee-up increments between 0° and 80° of sideslip followed by smaller lee-down increments at the higher angles of sideslip. As mentioned previously, the rolling characteristics of all configurations stem from the shape of the bow of the craft.

The spread of all the foregoing effects due to tunnel wind are summarized and presented in Figures 40 and 41.

6.3.2 INDIVIDUAL EFFECTS DUE TO BLOWING

The effects of blowing have been obtained for each configuration by taking the difference between measured characteristics in conditions of GWBS and GWS, when $C_{Q1} = 0.0365$.

The lift increments due to blowing are shown in Figure 28 where measured lift increments for each configuration have been offset plotted. Results for each configuration contain the lift due to cushion pressure. The differences between configurations are clouded by the probable lack of accuracy that has been discussed previously. The summarized results of Figure 40 have been corrected for cushion pressure effects.

The drag increments due to blowing are shown in Figure 29. All configurations show a decrease in drag in beamwind conditions as has been reported in Reference 2. The variation of drag with sideslip angles between 0° and 70° seems to be more pronounced with Configuration 1 than with the others. However, it is felt that these results may be impaired by lack of accuracy in drag measurement.

Figure 30 shows the effect of blowing on the pitching moment characteristics of all configurations. All configurations appear to be similarly affected and it is pointed out that the consistent nose-down contribution in headwind conditions and the consistent tail-up contribution in tailwind conditions stems from there being more cushion footprint area behind the axis of rotation than ahead of it.

The yawing moment increments due to blowing are shown in Figure 31 to be similar for all configurations. The general effect of blowing is one of destabilization.

The effects of blowing on the crosswind force characteristics of all configurations are shown in Figure 32. Results appear to be impaired by balance accuracy although certain trends are evidenced. With wind on the forward quarter, crosswind forces appear to decrease whereas with wind on the rear quarter, crosswind forces appear to increase.

The effects of blowing on rolling moments are shown for all configurations in Figure 33. All configurations are affected similarly with lee-down tendencies throughout the range of sideslip angles.

6.3.3 INDIVIDUAL EFFECTS DUE TO SUCTION

The effects of suction have been obtained for each configuration by taking the difference between measured characteristics in conditions of GWBS and GWB, when $C_{Q1} = 0.0365$.

The lift increments due to suction are shown in Figure 34. Particularly in the case of Configuration 1, there is evidence of lack of accuracy. Nevertheless, there is fair indication that there are no major differences between the effects on different configurations. All the data of Figure 34 includes a common error due to the inclusion of the negative lift associated with strut suction effects. This error has been corrected in the summarized effects of suction on lift in Figure 40. It will be seen that the general effect is one of increasing lift due to suction.

The effects of suction on the drag characteristics of all configurations are shown in Figure 35. In spite of some loss of confidence in the results for reasons of measurement accuracy, it will be noted that both Configurations 1 and 3 (and possibly Configuration 5) show evidence of suppression of separation from the rear of the top edge of the superstructure.

Increments of pitching moment due to suction for all configurations are shown in Figure 36. No particular trends are are in evidence and the spread of the data indicates that these suction effects are relatively small compared with those effects due to wind and blowing. This is shown in Figure 40.

The effect of suction on the yawing moment characteristics of all configurations is shown in Figure 37. It will be noted that Configurations 1 and 3 exhibit characteristics which differ from those of the other configurations. These two configurations show definite destabilizing effects over most of the sideslip

range, once again pointing to separation effects in the vicinity of the rear quarter of the superstructure. Other configurations indicate little effect when the wind is on the forward quarter, and with wind in a near tailwind condition, effects are random.

Increments of crosswind force coefficient due to suction are shown in Figure 38 for all configurations. Configuration 1 shows a decrease in crosswind force for wind on the forward quarter, but when the wind is on the rear quarter there is an increase in crosswind force. Other configurations show smaller decreases in crosswind force when the wind is on the forward quarter. When the wind is on the rear quarter, no particular trend is in evidence.

The effect of suction of the rolling moments of all configurations are shown in Figure 39. The general effect on all configurations is small - a lee-down increment when induction ports are in the rear of the superstructure; and a lee-up increment when the ports are forward.

7. CONCLUSIONS

7.1 TECHNIQUE

Before discussing such conclusions as may be drawn from this study of the effect of lift-system airflow on the hull aerodynamics of hovercraft, it is considered desirable to pass comment on the technique employed during the test programme and to point out such limitations as are believed extant.

As has been reported in previous work on the subject of hull aerodynamics, experimentation involves the measurement of forces and moments in conditions of intense separation. Many such separations originate simultaneously from differing sources around the hull, probably with random phasing at frequencies related to tunnel speed. Hence the environment is highly unsteady and it requires the use of a balance having relatively long time constants in order that forces and moments may be averaged during measurement.

The balance employed during this test programme has long time constants by virtue of the high mass of its mechanical components. However, the balance was designed for forces and moments of far greater magnitude than those generated by the hovercraft model. Inevitably, some lack of accuracy might be anticipated in these conditions and it is surprising, particularly so in the case of lift forces, that such repeatable results were obtained in no-flow conditions. It would suggest that the averaging capability of the balance was adequate for the task, and was free from mechanical constraints imposed by the vacuum system.

However, in conditions of lift-system airflow with combined blowing and suction, and with independent blowing and suction, measurements of lift and drag forces (and to a lesser extent those of crosswind force) are quite obviously of questionable accuracy in certain instances. A possible explanation for these inaccuracies might be that the lift-system airflow into induction ports and from beneath the skirt of the model is also unsteady as far as the aerodynamics of the hull is concerned, although not as far as the pipe-flow in the air measuring systems concerned.

Independent preliminary tests of the blowing and suction systems showed no evidence of unsteady flow, and therefore any unsteadiness during tunnel testing must be attributed to aerodynamic effects. These effects, might be thought of as follows. In the case of efflux from beneath the skirt, it could be that at some particular point on the skirt perimeter the discharge is not constant but varies at some frequency appreciably lower than separation frequencies which have been shown to have little effect on balance accuracy. The variation in local discharge may be thought of as being a wave of discharge passing down the length of the skirt, or a cyclic change of hovergap due to mechanical deformation.

In the case of unsteadiness in induction, all configurations had two induction ports and there is possibly crossflow between these ports again at frequencies which cause unsteadiness and loss of accuracy in measurement. This is akin to the low frequency rumbling which occurs when the front windows of a car are partially open at certain speeds. In this instance, the rumbling is almost identifiable to the human ear as discrete pulses of pressure.

The foregoing is certainly nothing more than hypothesis but it is suggestive that a more fundamental understanding of the effects of lift-system airflow should be sought with techniques and equipment more suited to the test than has been possible in this programme

7.2 EFFECTS OF LOCATION OF INDUCTION PORTS

Most of the effects of location of induction ports on the aerodynamic characteristics of the hovercraft must be considered to be of second order. Apart from the HD-2 configuration, no other location for induction ports appears to have marked superiority over any other location. Definite trends, but not ones of major consequence, are as follows.

(i) Lift forces appear to increase as induction ports are moved forward on the superstructure.

(ii) The drag levels of the HD-2 configuration are beneath those for the other configurations and appear to be intimately related to the degree of separation originating from the rear of the superstructure. However, the tests have not been sufficiently accurate to establish the relative importance of form drag and momentum drag.

(iii) The pitching moments become progressively nose-up as the location of the induction ports move forward on the superstructure.

(iv) The rolling moments tend to become more lee-down in sense as induction port locations move forward.

7.3 COMPARATIVE EFFECTS OF WIND, BLOWING AND SUCTION

The effect of wind on the basic shape of the HD-2 hovercraft has been well established and confidence can be placed in the results obtained during the test programme. For reasons discussed previously, there is evidence of lack of accuracy in the lift, drag and crosswind measurements in conditions of blowing and suction, both independently and in combination. Nevertheless, while the absolute values of effects due to airflow may be open to question, certain definite trends have been established.

(i) The aerodynamic characteristics of a particular hovercraft shape are primarily due to the shape itself, and that the lift-system airflow through that shape does not affect those characteristics to any major degree of consequence.

(ii) There is evidence that the individual effect of blowing is to decrease the lift, whereas the individual effect of suction is to increase that lift. In combination, at the low flow rate the individual effects cancel; whereas at the high flow rate the loss of lift due to blowing is greater than the increase due to suction.

(iii) The most clearly defined effect of blowing is a decrease of drag in beamwind conditions. There is evidence of an increase in drag in headwind and tailwind conditions due to mixing of the cushion efflux with the free stream. The most pronounced effect of suction on the drag characteristics occurs when wind is on the forward quarter and is due to the suppression of separation from the rear of the superstructure. Limitations in the accuracy of the drag measurements of this programme

preclude any specific comments on the relative magnitude of the two effects.

(iv) Pitching moments due to the cushion footprint when blowing appear to be predictable and far more significant than the small nose-down contribution due to suction.

(v) The basic unstable yawing moment of the hull shape is further destabilized, possibly about 50%, by the effects of blowing and suction.

(vi) Crosswind forces on the basic hovercraft shape can be affected by as much as 50% due to the effects of blowing and suction. In general, the trend is a reduction of force when the wind is on the forward quarter and an increase in force when the wind is on the rear quarter.

(vii) Rolling moments due to blowing can cause a lee-down change in moment throughout the sideslip range. This lee-down change can be as great as the maximum lee-up moment due to the basic shape of the hovercraft. The effect of suction is insignificant.

7.4 EFFECTS ON HANDLING QUALITIES

None of the effects of the lift-system airflow on the aerodynamic characteristics of the hull are of major consequence as far as the handling qualities of hovercraft are concerned.

From this research programme and the two previous research programmes reported in References 1 and 2, it is abundantly clear that second order refinement in design is obtainable by giving careful consideration to means for the suppression of separation from the hull and superstructure. As pointed out in Reference 1, this can be achieved by the use of generous radii along the horizontal and vertical edges of the basic components of the configuration.

Of second order importance only, is the location of induction ports. There are indications that rear locations are preferable to forward ones. However, it is considered that further research with improved technique into the effects of separation on lift and drag characteristics combined with research into the effects of pressure recovery on the lift-system airflow might modify the above preliminary conclusion.

8. LIST OF REFERENCES

1. E.J. Andrews — The Aerodynamic Characteristics of a Family of Related Hovercraft Shapes. College of Aeronautics Memo No. 133, September 1967.

2. C.J. Richards — The Effect of Cushion Efflux on the External Aerodynamics of a Model Hovercraft. College of Aeronautics Thesis, September 20th, 1968.

3. Anon. — Methods for the Measurement of Fluid Flow in Pipes. Part 1. Orifice Plates, Nozzles and Venturi Tubes. B.S. 1042, Part 1, 1964.

4. M.V. Herbert, D.L. Martlew and R.A. Pinker — The Design-point Performance of Model Internal-expansion Propelling Nozzles with Area Ratios up to 4. R. & M. 3477, December 1963.

5. J. Williams and S.F.J. Butler — Further Developments in Low-speed Wind-tunnel Techniques for V/STOL and High-lift model Testing. R.A.E. Tech. Note Aero. 2944, January 1964.

6. Anon. — Note on the Calibration of 8ft x 6ft Wind-tunnel Balance. Internal Note, College of Aeronautics, September 1962.

9. LIST OF FIGURES

Figure 22. Wind, lift increment due to, at $C_{Q1} = 0.0365$.

23. Wind, drag increment due to, at $C_{Q1} = 0.0365$.

24. Wind, pitching moment increment due to, at $C_{Q1} = 0.365$.

25. Wind, yawing moment increment due to, at $C_{Q1} = 0.365$.

26. Wind, crosswind force increment due to, at $C_{Q1} = 0.0365$.

27. Wind, rolling moment increment due to, at $C_{Q1} = 0.365$.

28. Blowing, lift increment due to, at $C_{Q1} = 0.0365$.

29. Blowing, drag increment due to, at $C_{Q1} = 0.0365$.

30. Blowing, pitching moment increment due to, at $C_{Q1} = 0.0365$.

31. Blowing, yawing moment increment due to, at $C_{Q1} = 0.0365$.

32. Blowing, crosswind force increment due to, at $C_{Q1} = 0.0365$.

33. Blowing, rolling moment increment due to, at $C_{Q1} = 0.0365$.

34. Suction, lift increment due to, at $C_{Q1} = 0.0365$.

35. Suction, drag increment due to, at $C_{Q1} = 0.0365$.

36. Suction, pitching moment increment due to, at $C_{Q1} = 0.0365$.

37. Suction, yawing moment increment due to, at $C_{Q1} = 0.0365$.

38. Suction, crosswind force increment due to, at $C_{Q1} = 0.0365$.

39. Suction, rolling moment increment due to, at $C_{Q1} = 0.0365$.

Figure 40.
41. } Individual effects of wind, blowing and suction at C_{Q1} = 0.0365.

42. Effects of port location at C_{Q1} = 0.0365.

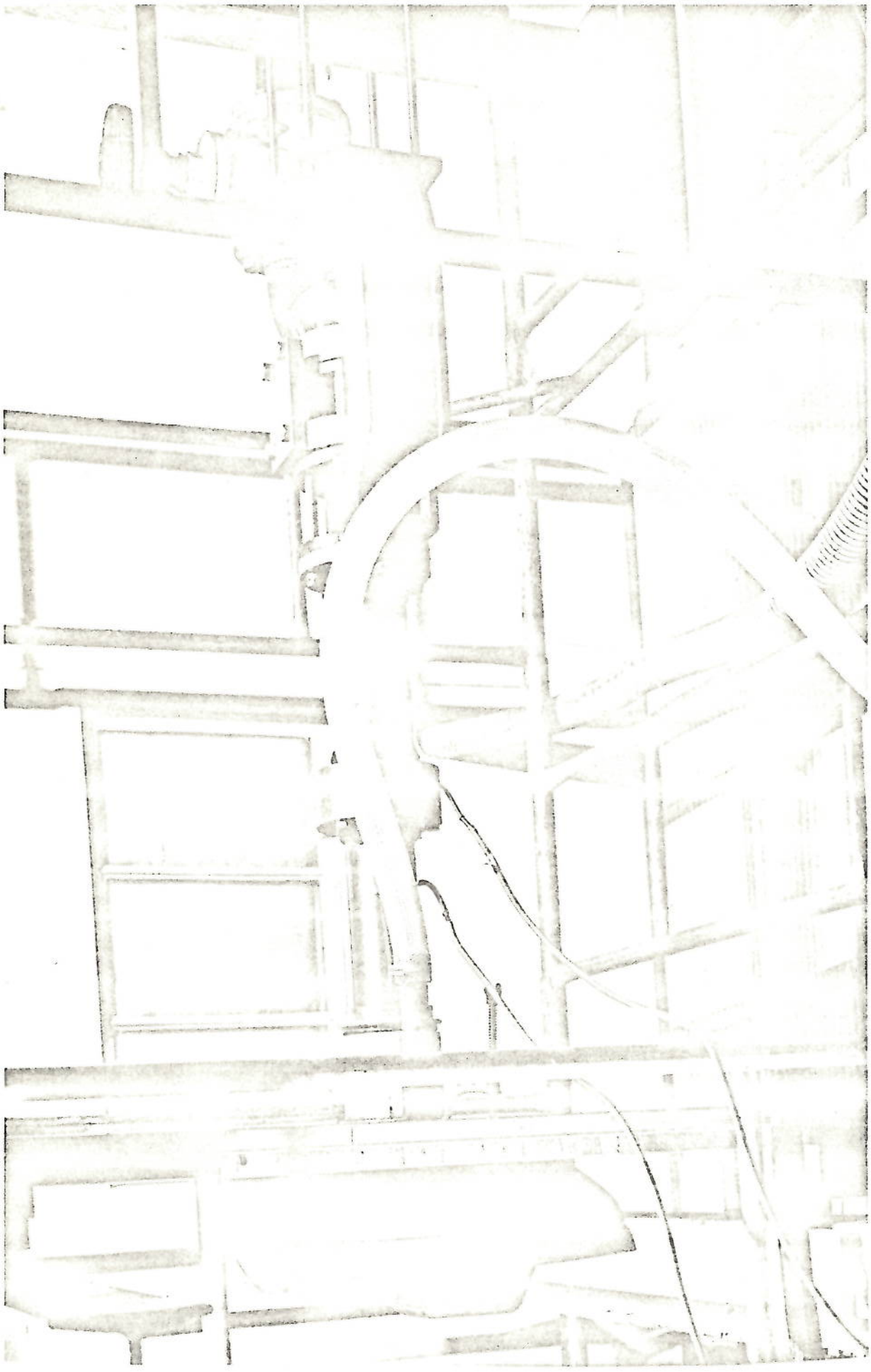

FIG. 1. STATIC TEST FACILITY.

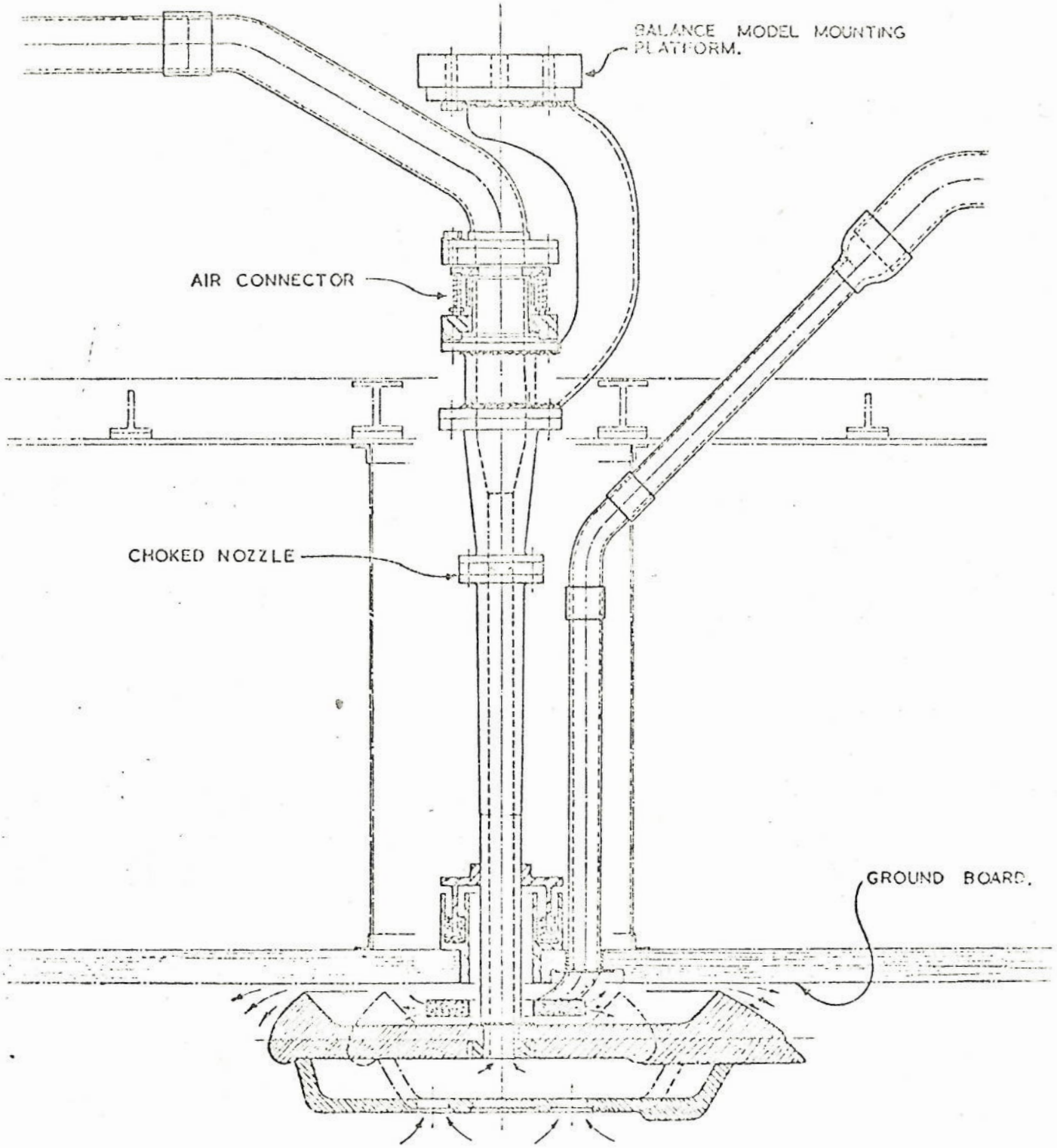

FIG. 2. HOVERCRAFT TEST FACILITY.

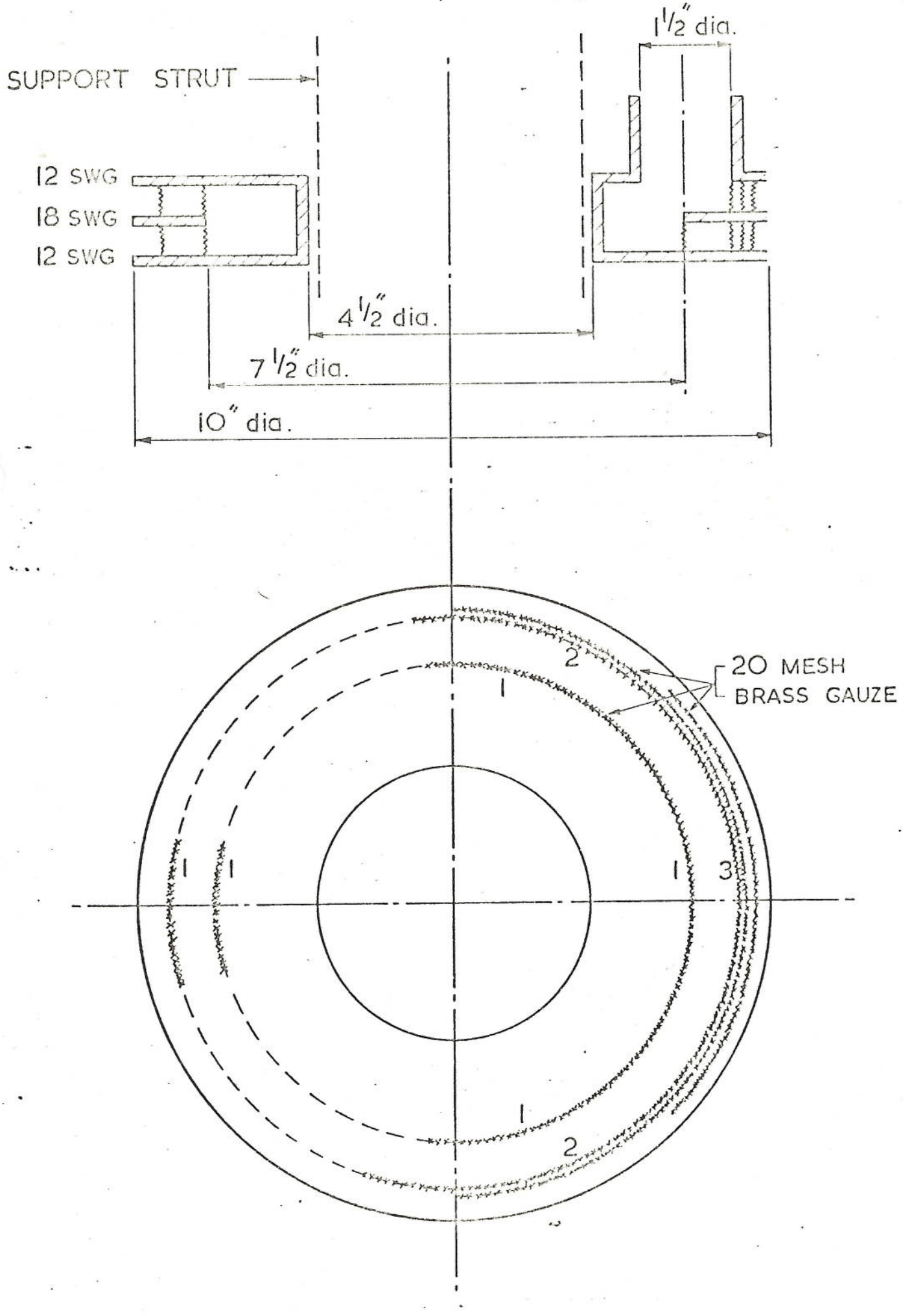

FIG. 3. COMPRESSED AIR DISTRIBUTOR

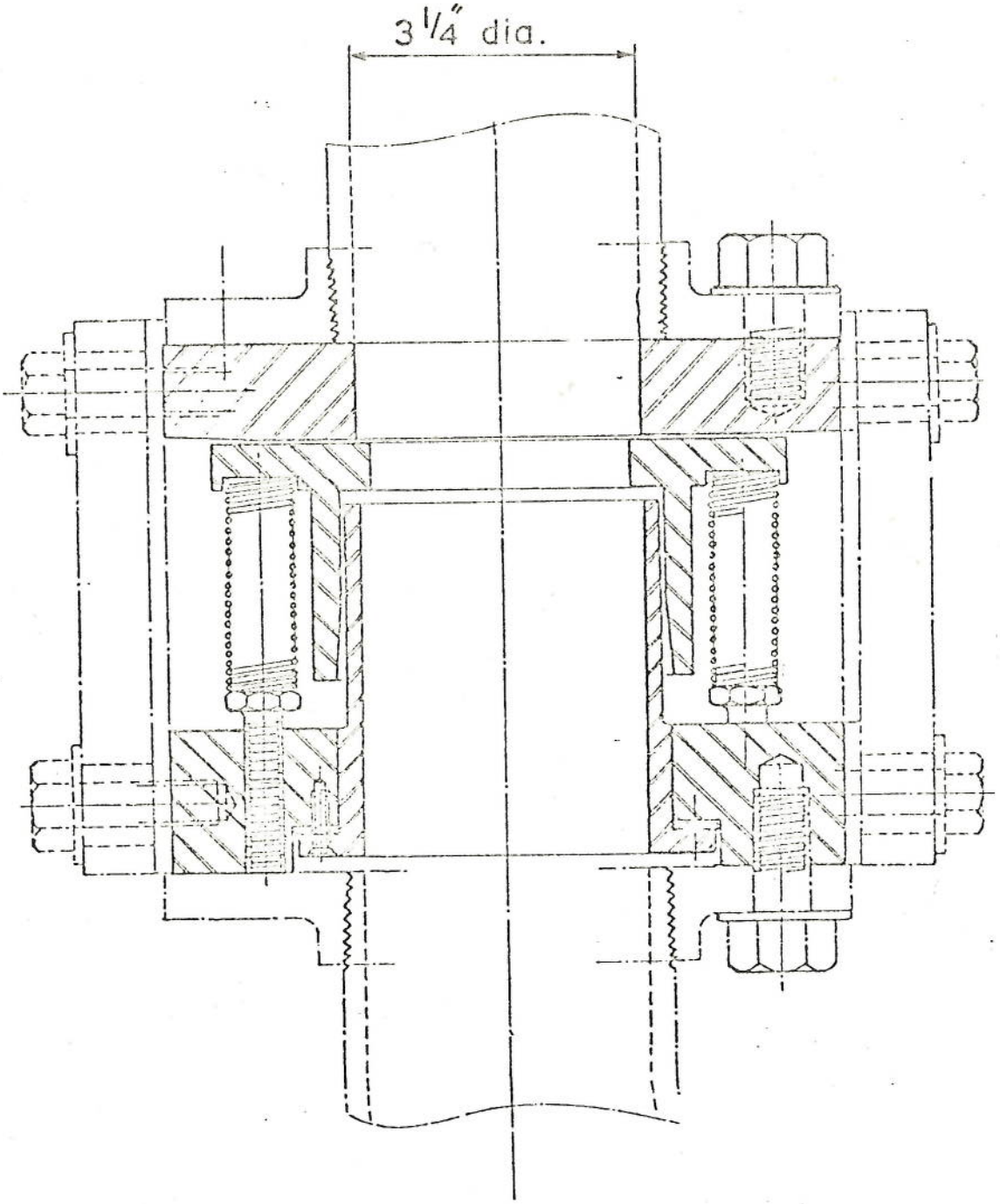

FIG. 4. AIR CONNECTOR.

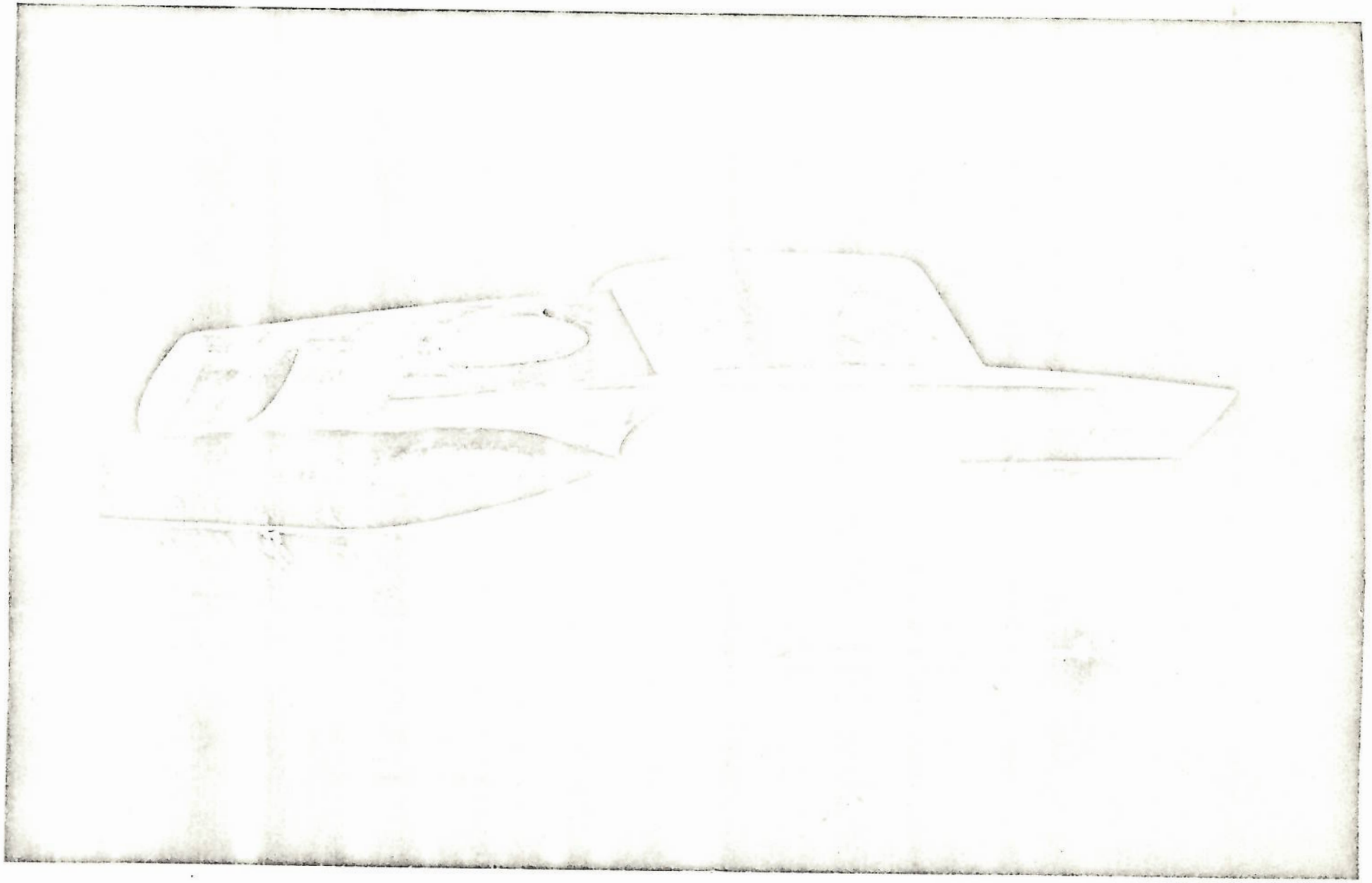

FIG. 5. HD-2 MODEL WITH HOLLOW SUPERSTRUCTURE.

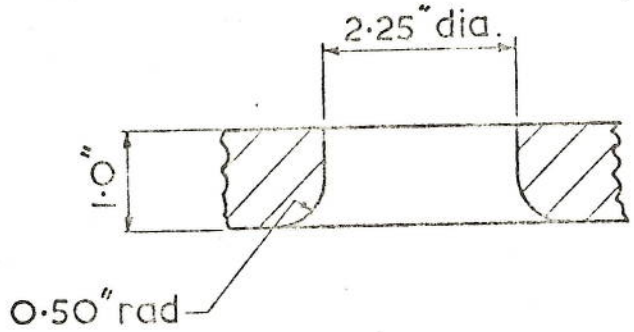

DETAIL OF PORT PROFILE

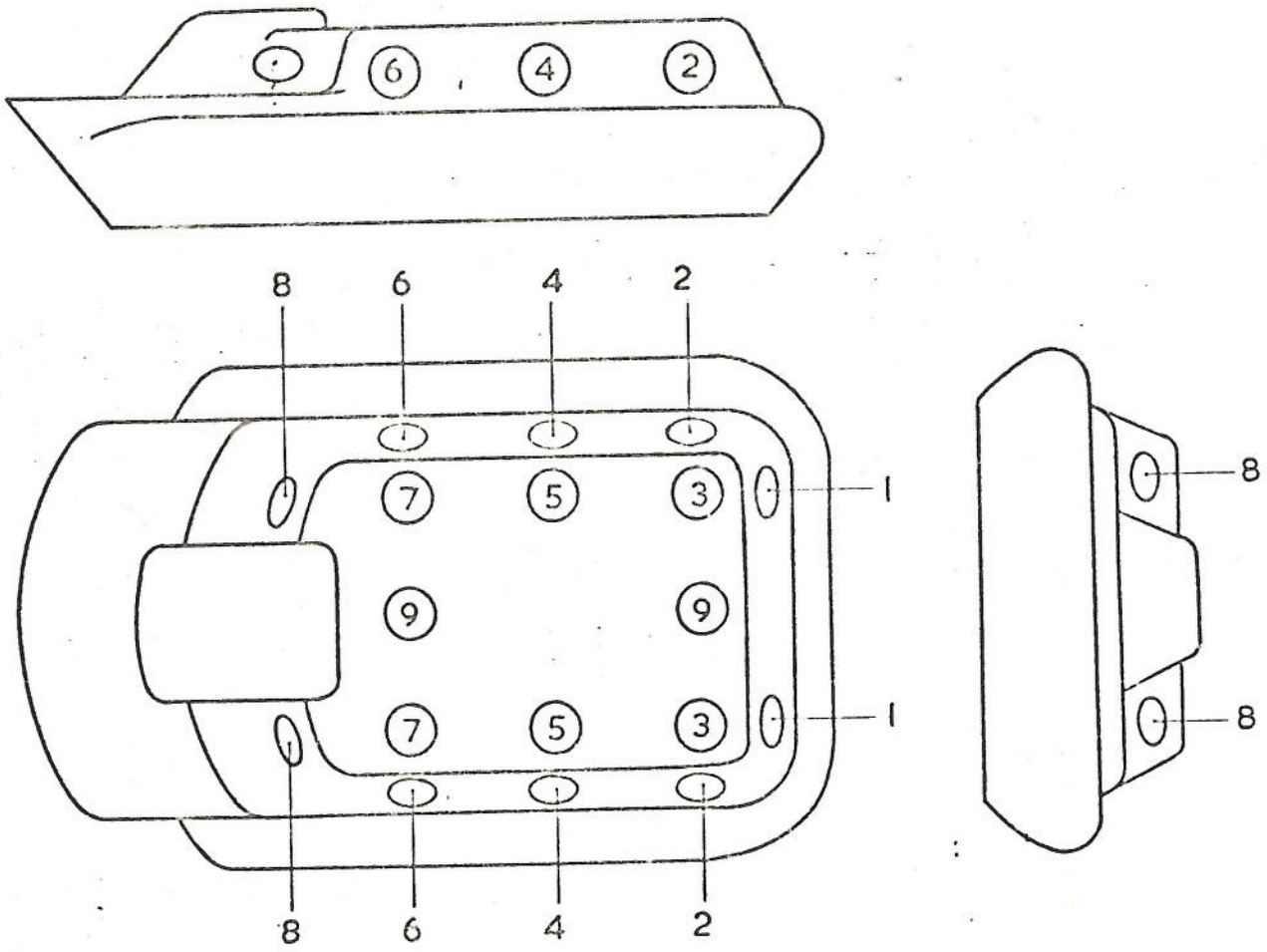

CONFIGURATION 1 - HD-2

FIG. 6. INDUCTION PORT LOCATION AND DETAIL.

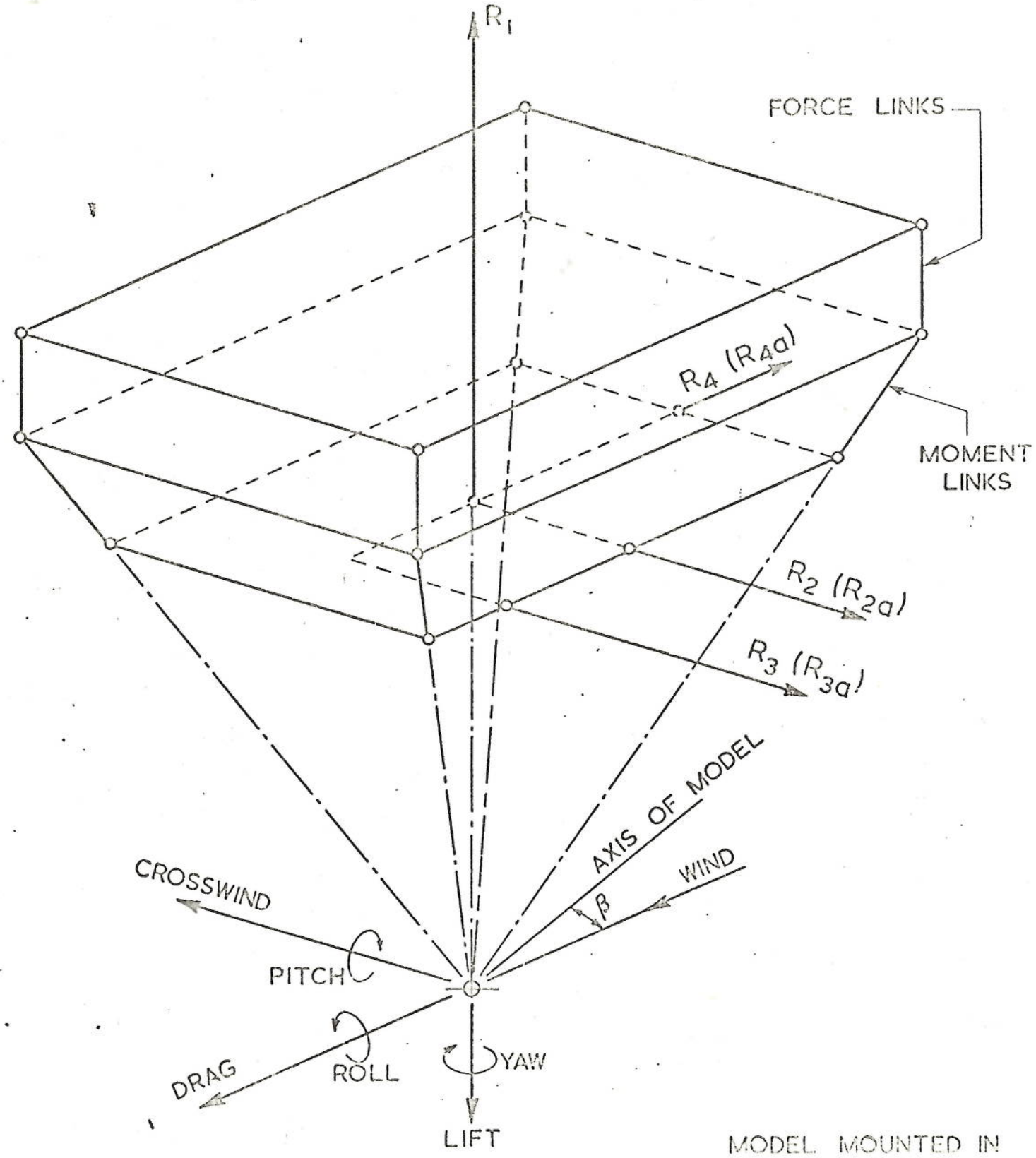

FIG.7. SIGN CONVENTION – BALANCE SYSTEM.

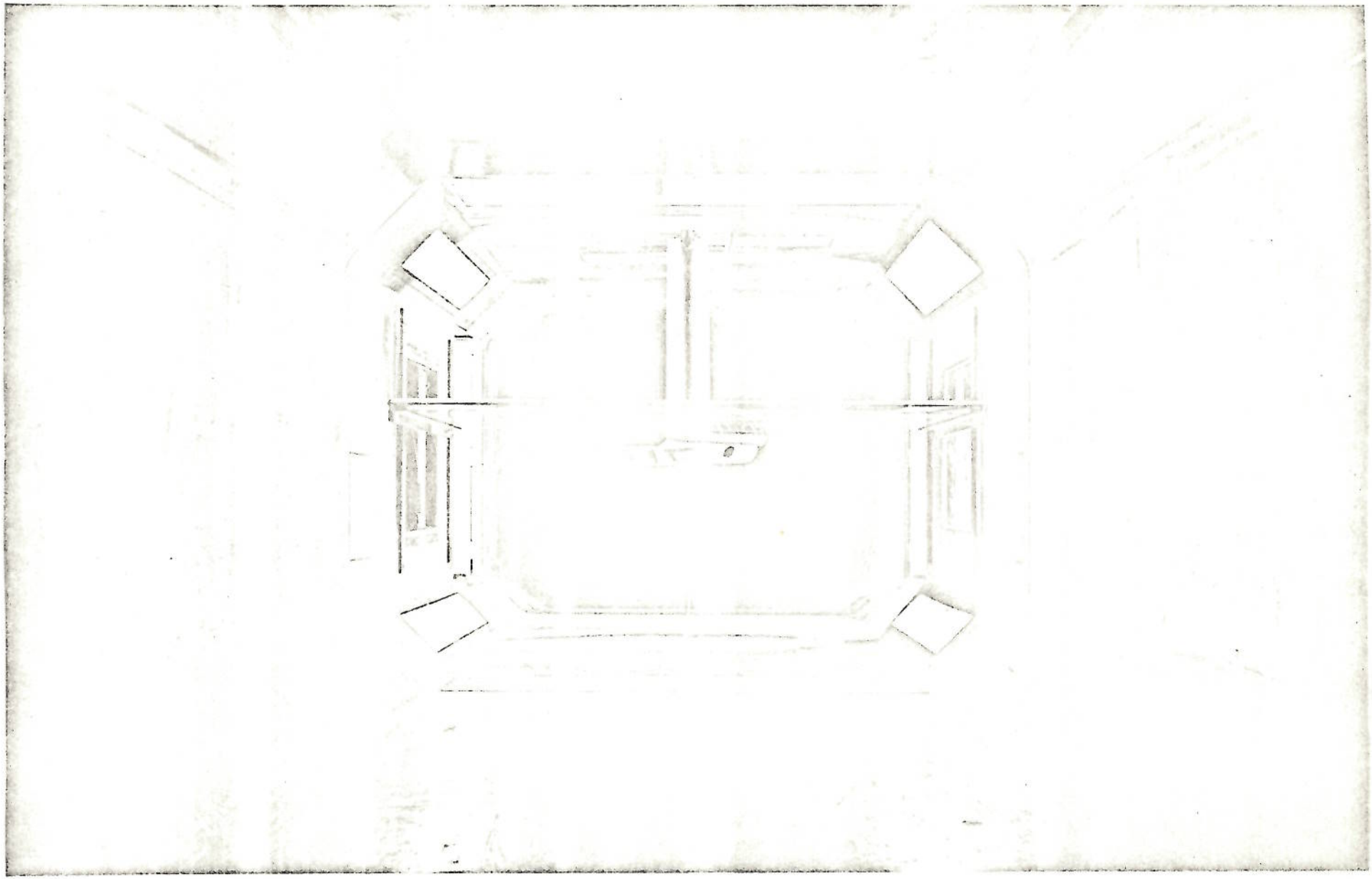

FIG. 8. HD-2 WIND-TUNNEL INSTALLATION.

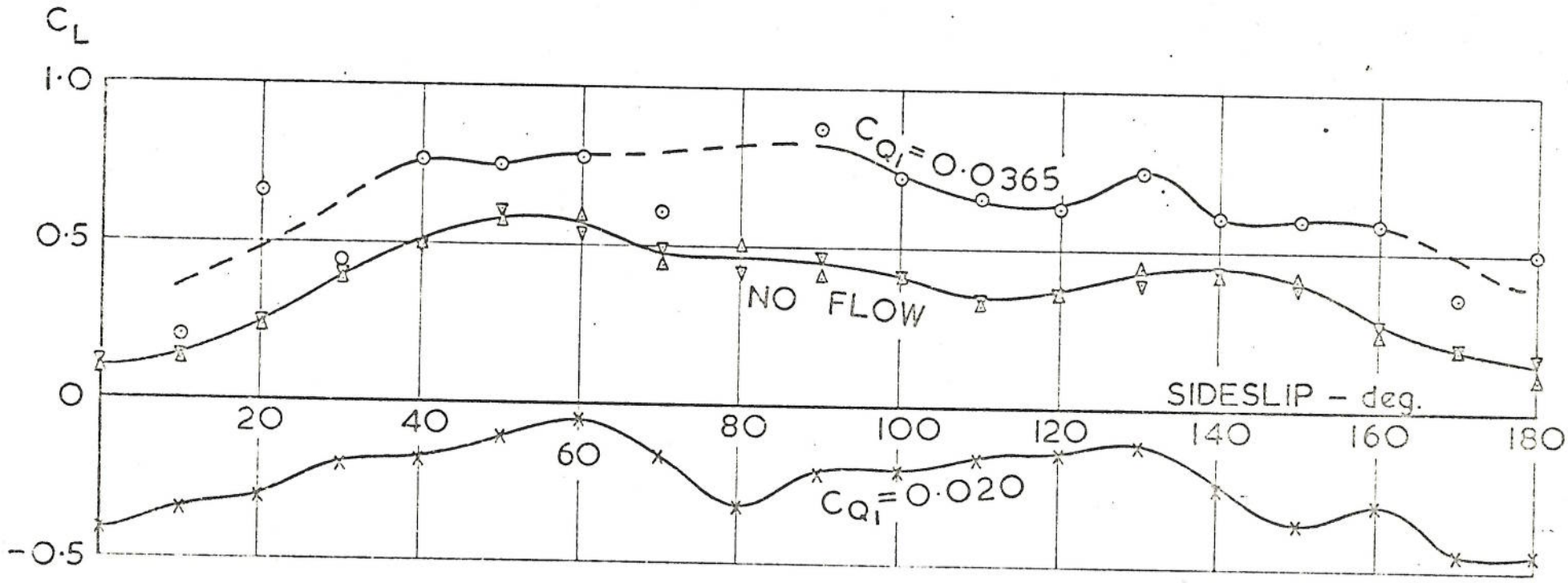

FIG. 9. MEASURED LIFT COEFFICIENT. CONFIGURATION 1-HD-2.

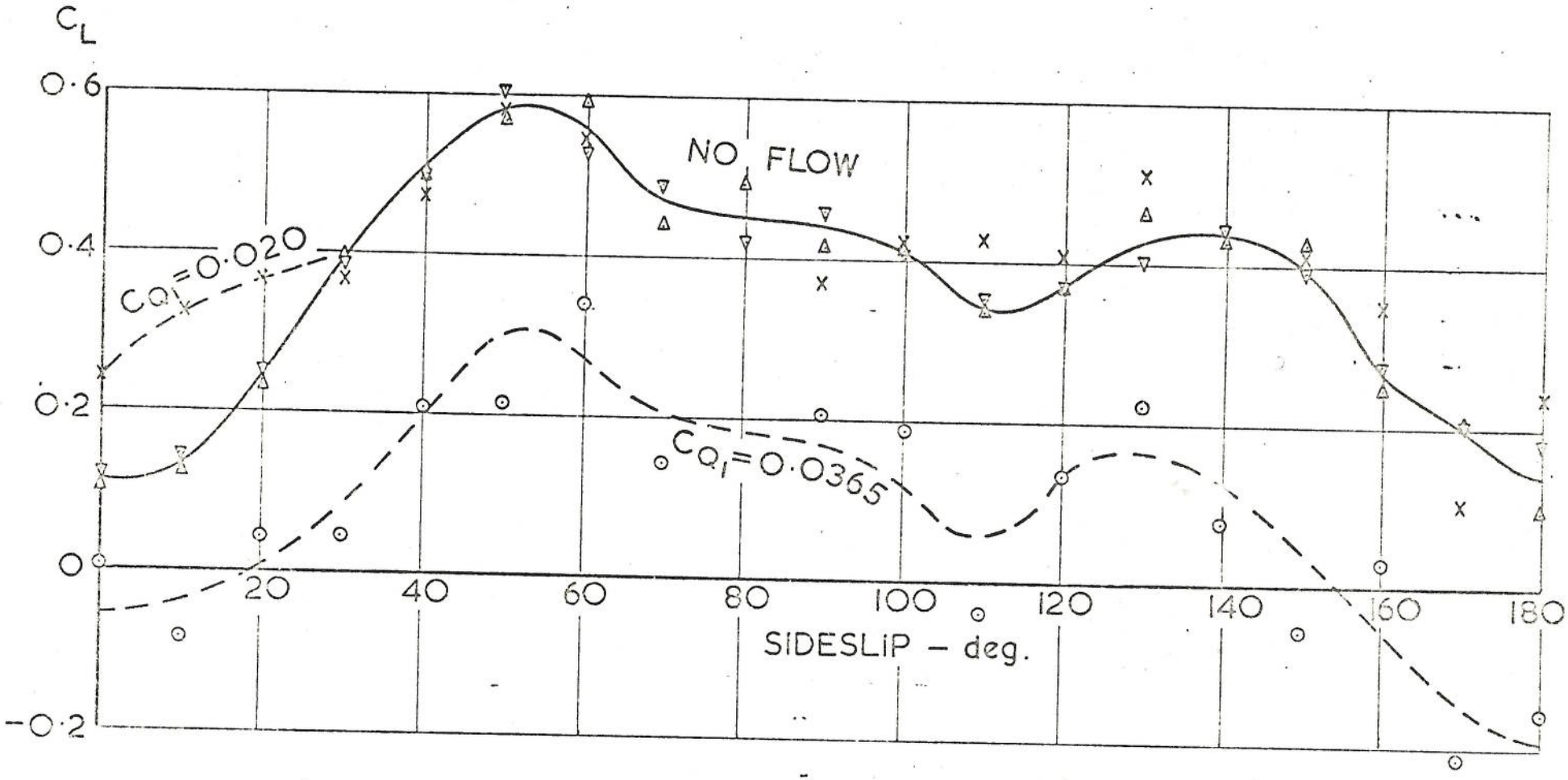

FIG. 10. LIFT COEFFICIENT, CORRECTED. CONFIGURATION 1–HD-2

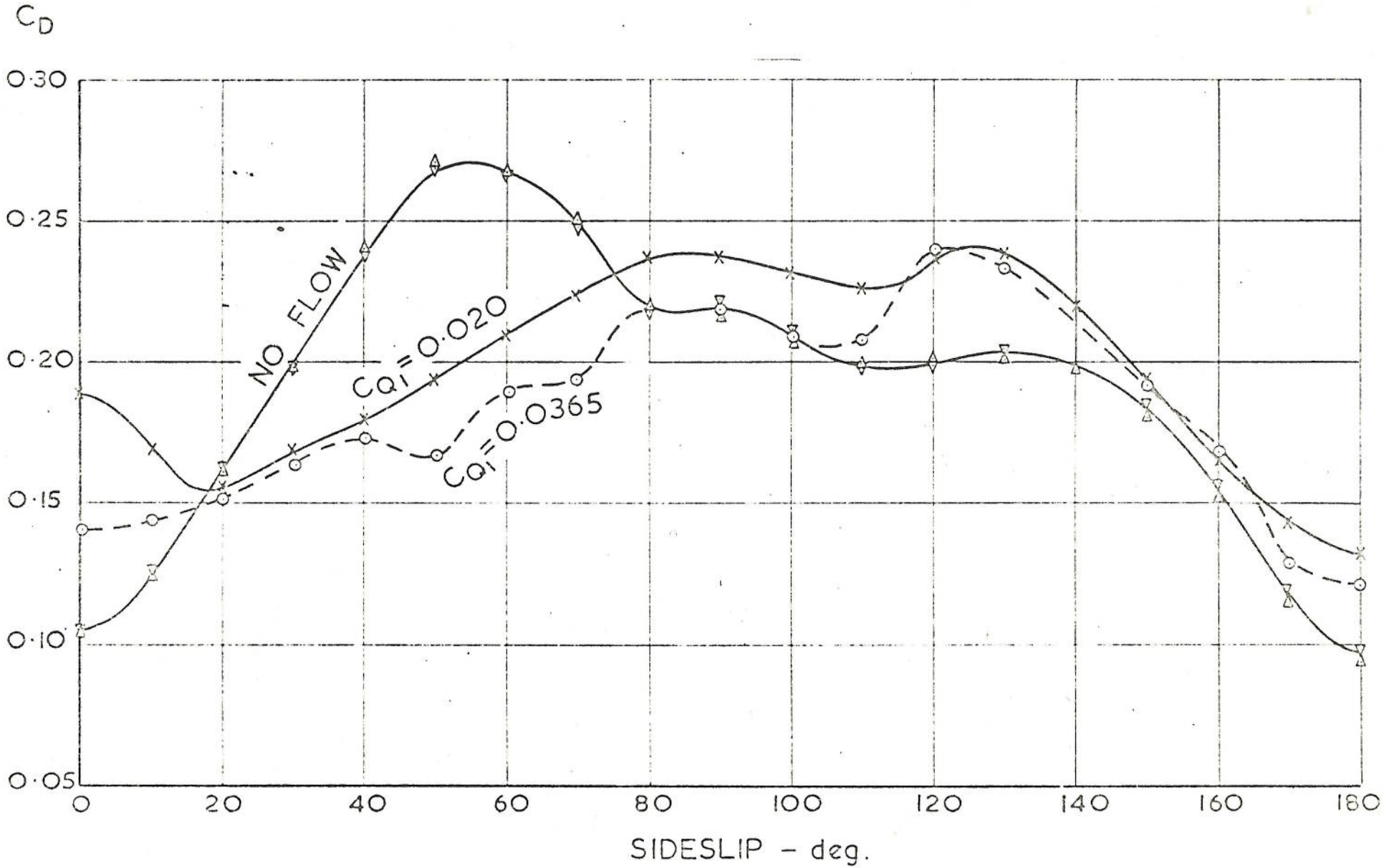

FIG. 11. DRAG COEFFICIENT. CONFIGURATION 1 – HD-2.

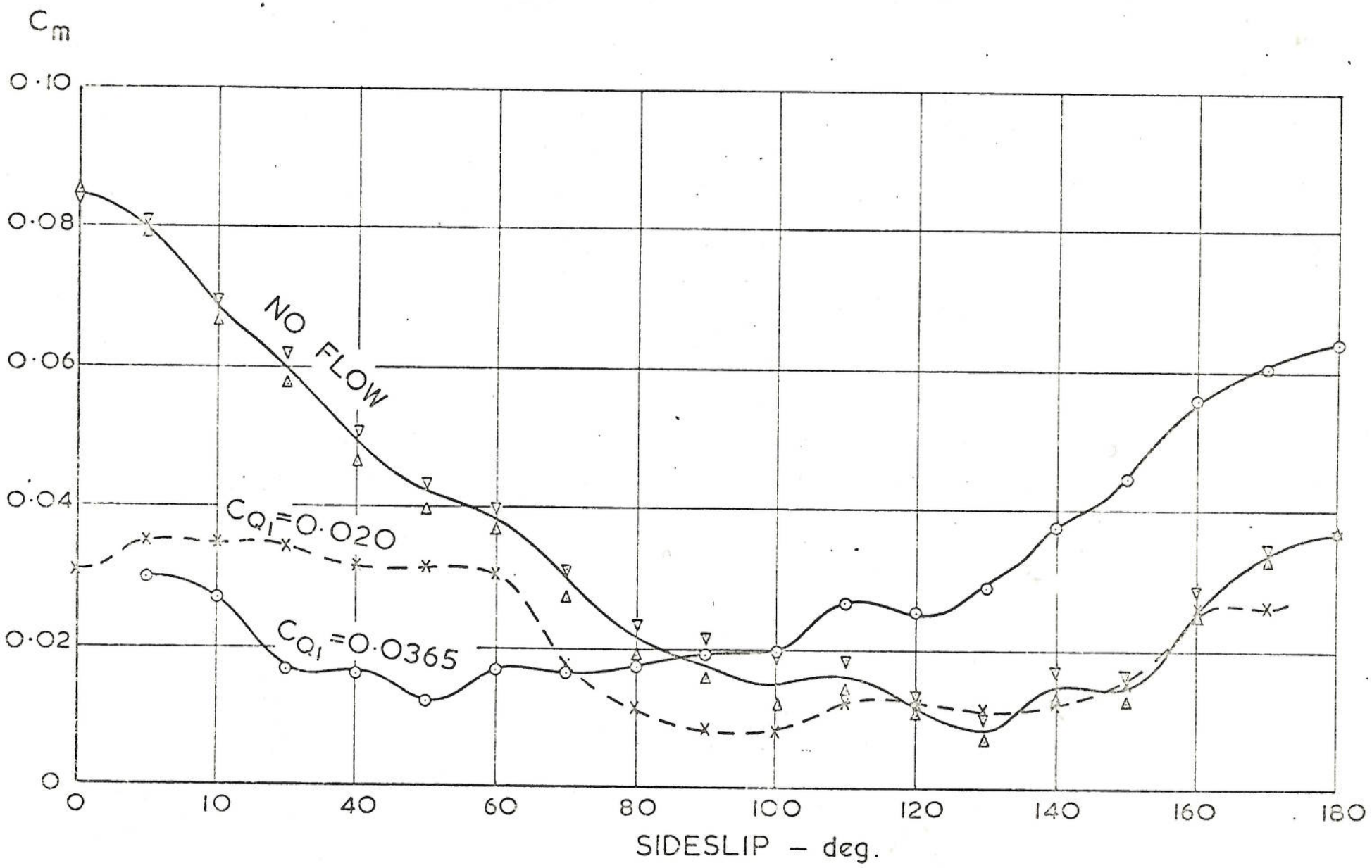

FIG. 12. PITCHING MOMENT COEFFICIENT. CONFIGURATION 1-HD-2.

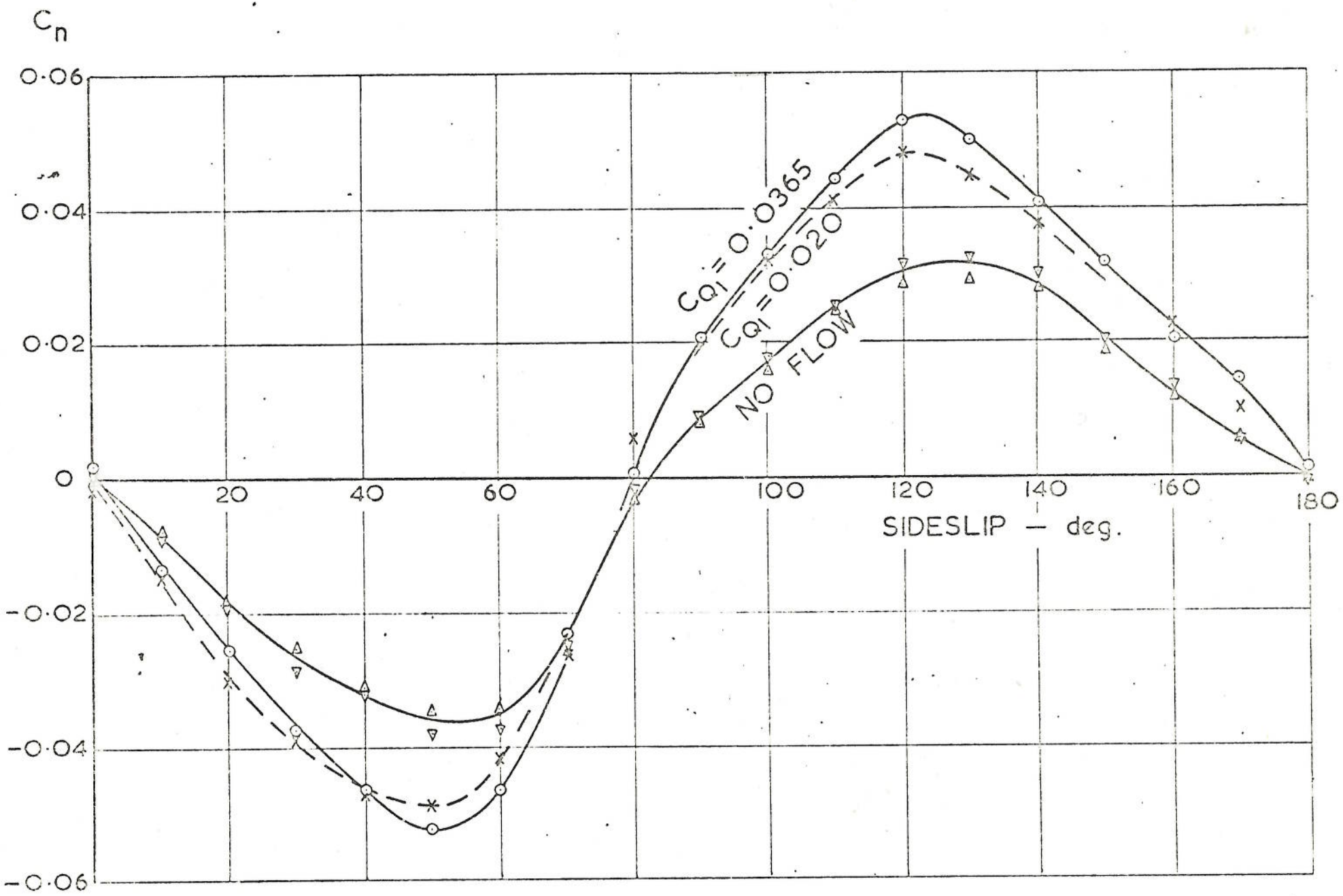

FIG. 13. YAWING MOMENT COEFFICIENT. CONFIGURATION 1—HD-2

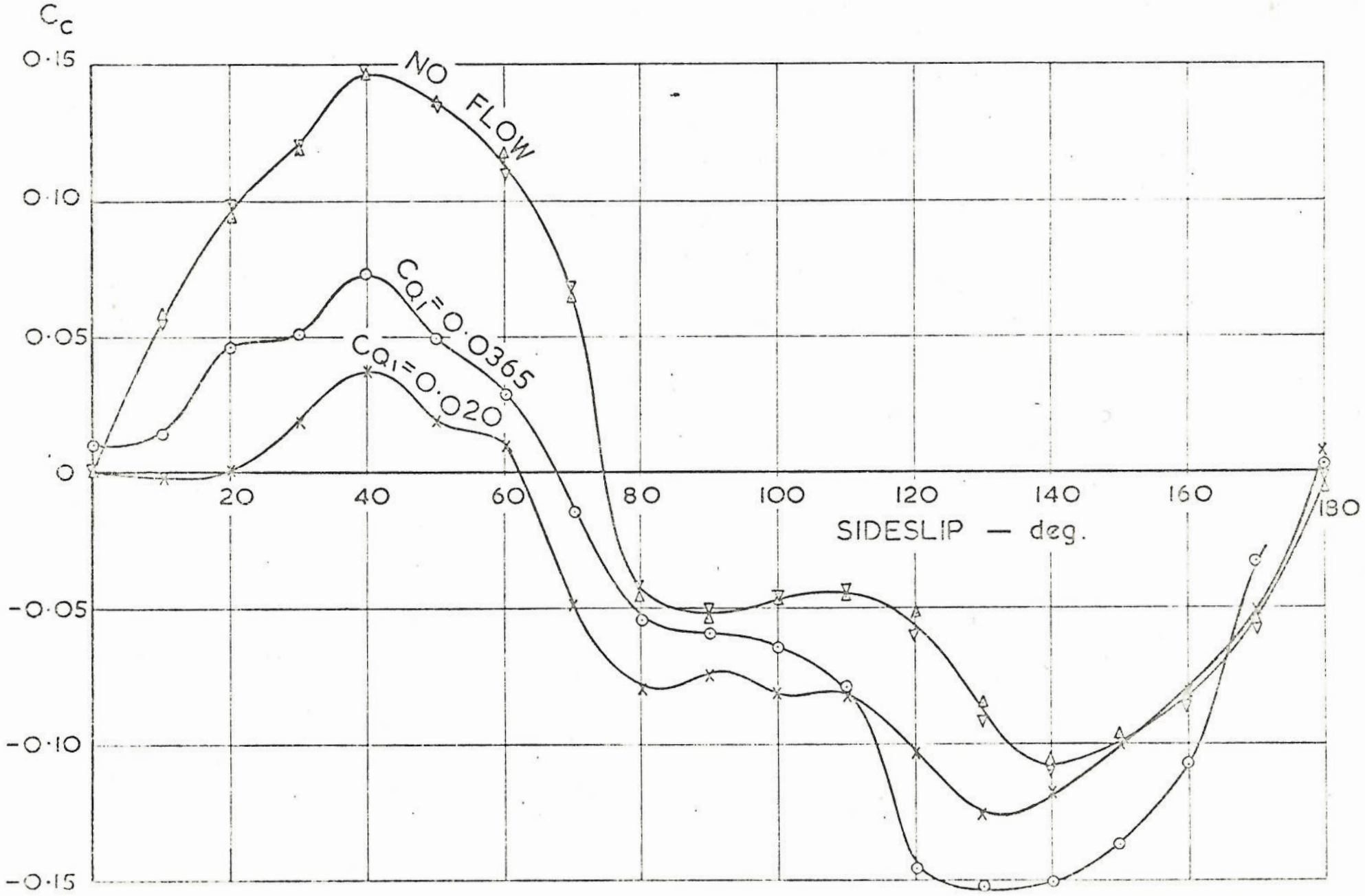

FIG. 14. CROSSWIND FORCE COEFFICIENT. CONFIGURATION 1 — HD-2

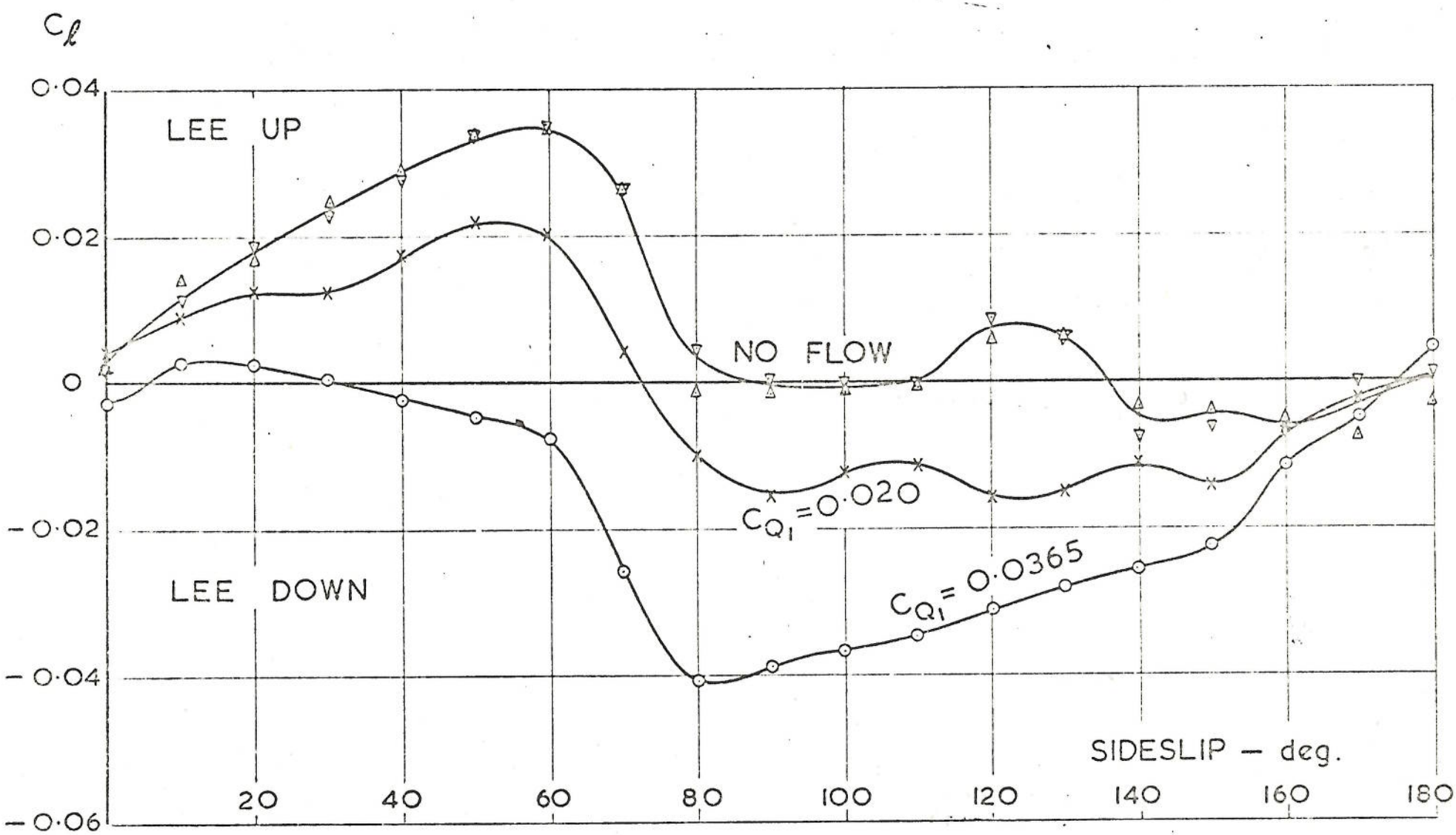

FIG. 15. ROLLING MOMENT COEFFICIENT. CONFIGURATION I — HD-2

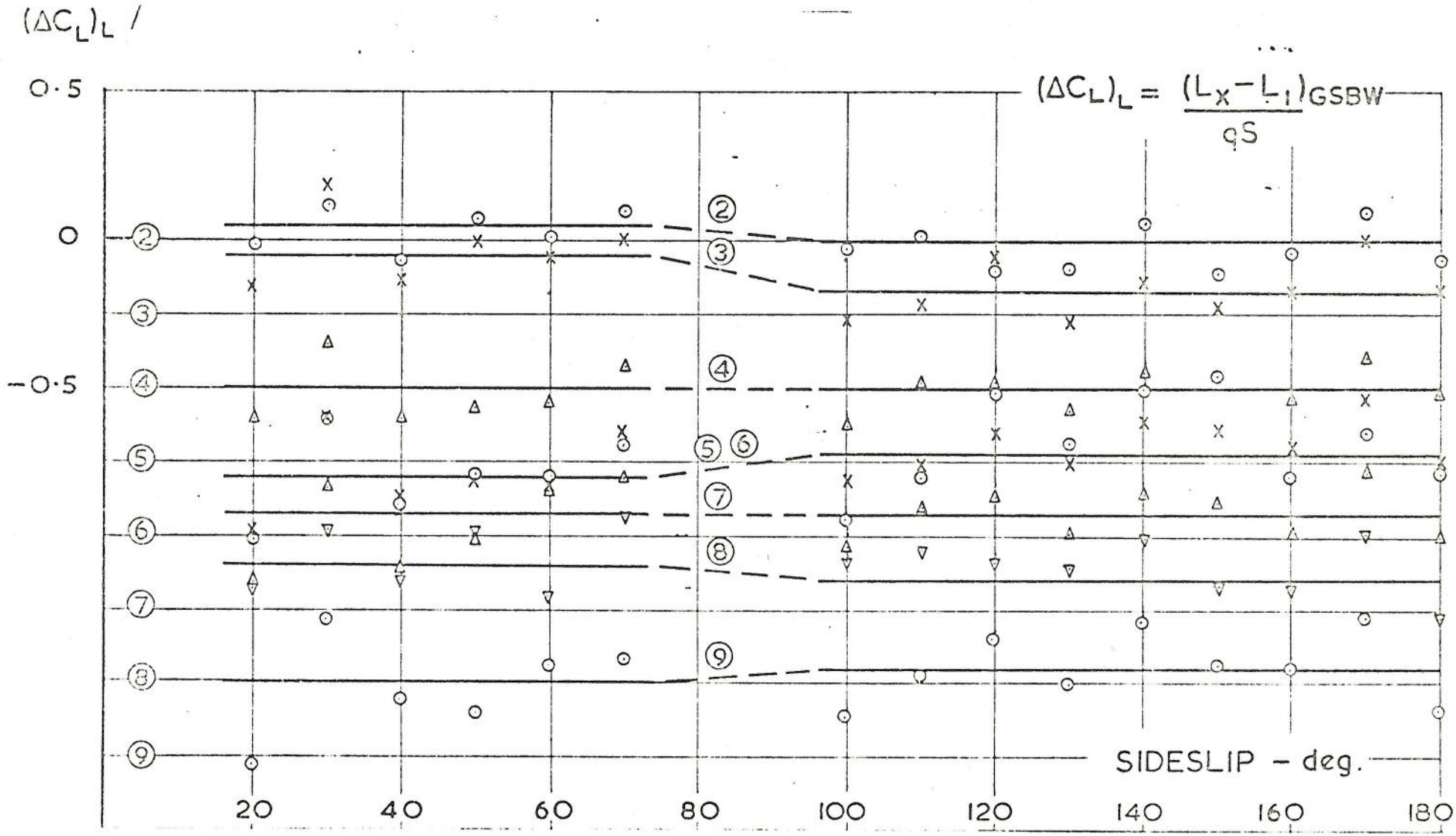

FIG. 16. LIFT INCREMENTS DUE TO PORT LOCATION. $C_{Q_1} = 0{\cdot}0365$

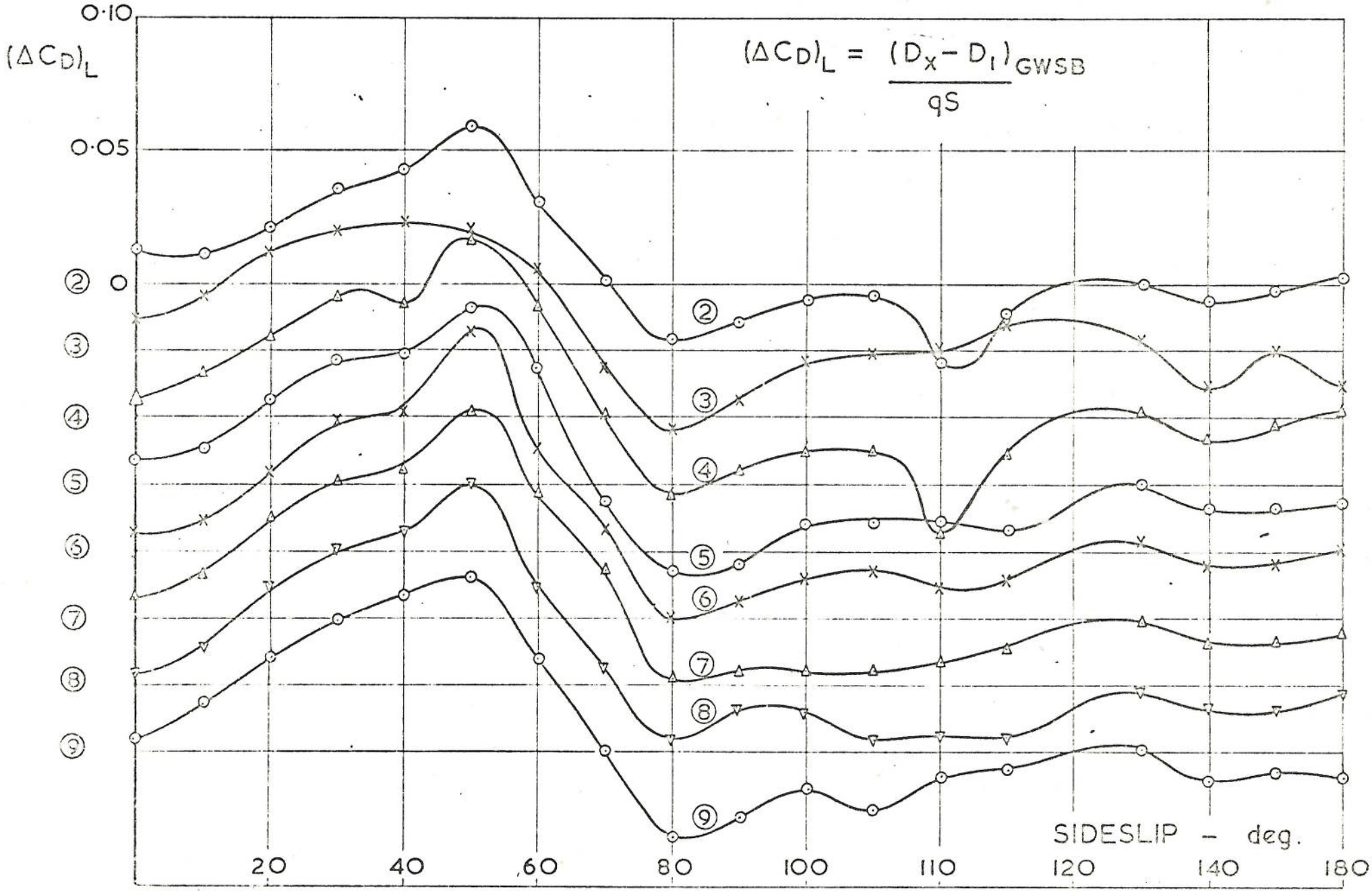

FIG. 17. DRAG INCREMENT DUE TO PORT LOCATION. $C_{Q_1} = 0·0365$

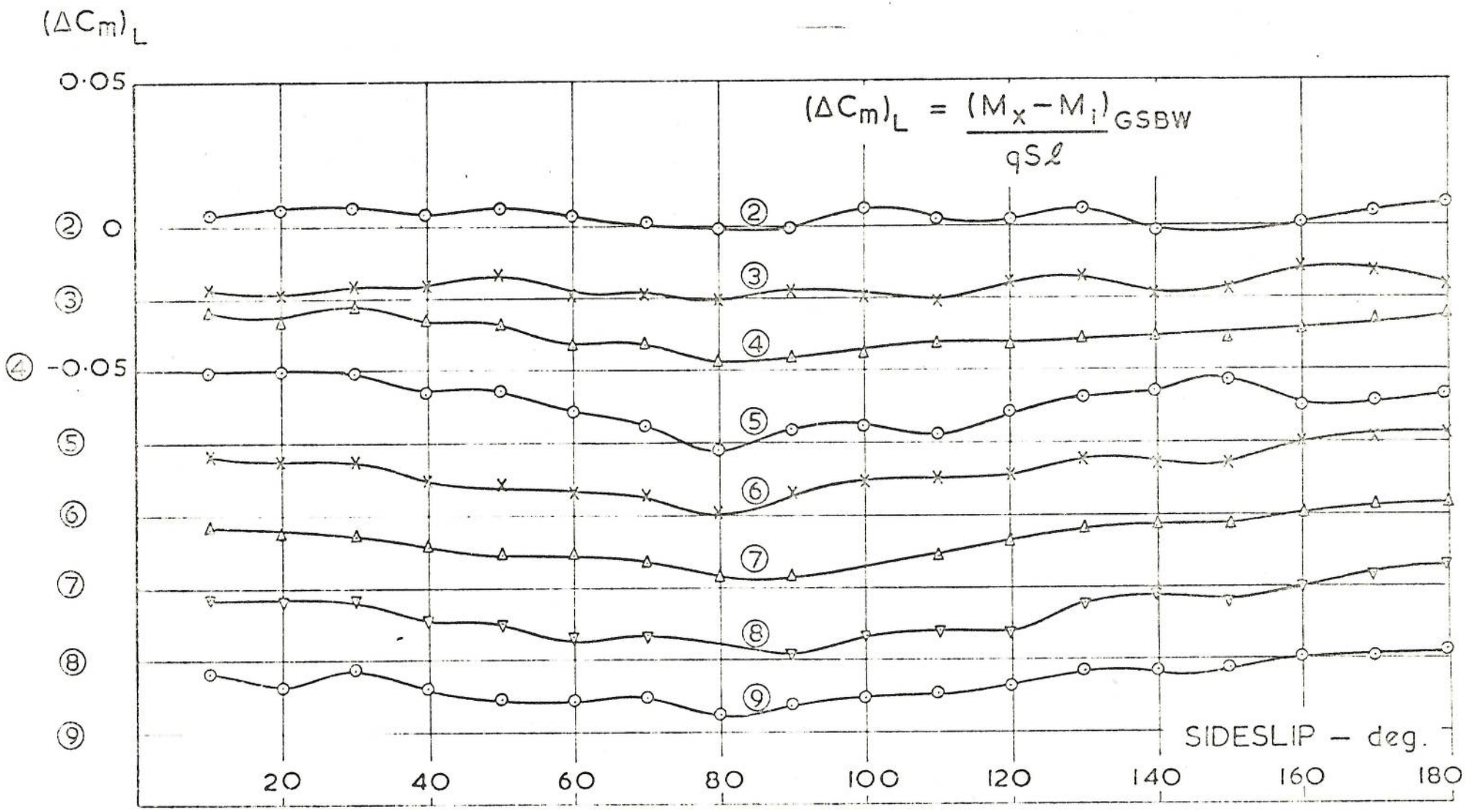

FIG. 18. PITCHING MOMENT INCREMENT DUE TO PORT LOCATION.

$C_{Q_1} = 0·0365$

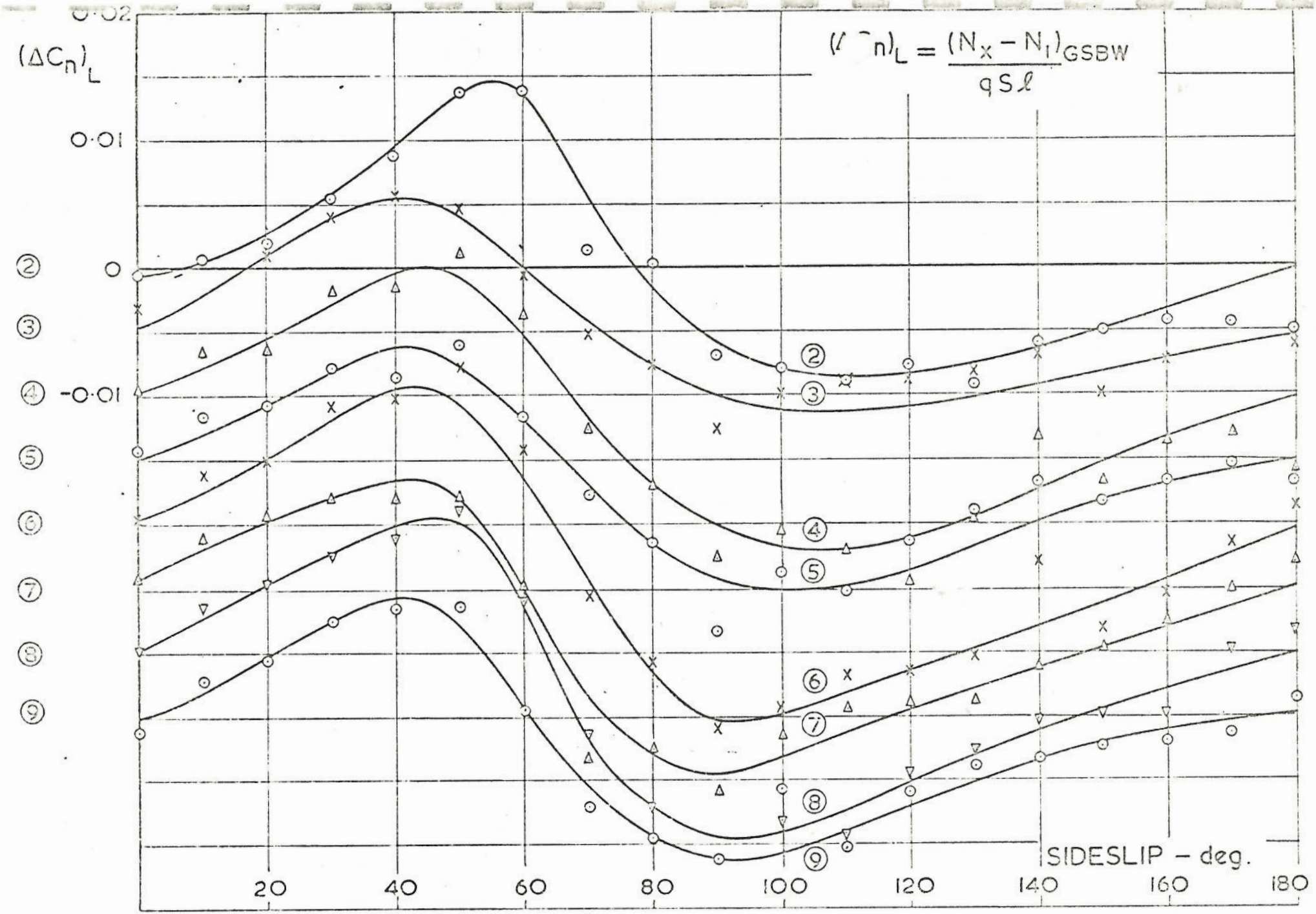

FIG. 19. INCREMENT OF YAWING MOMENT DUE TO PORT LOCATION.

$C_{Q_1} = 0·0365$

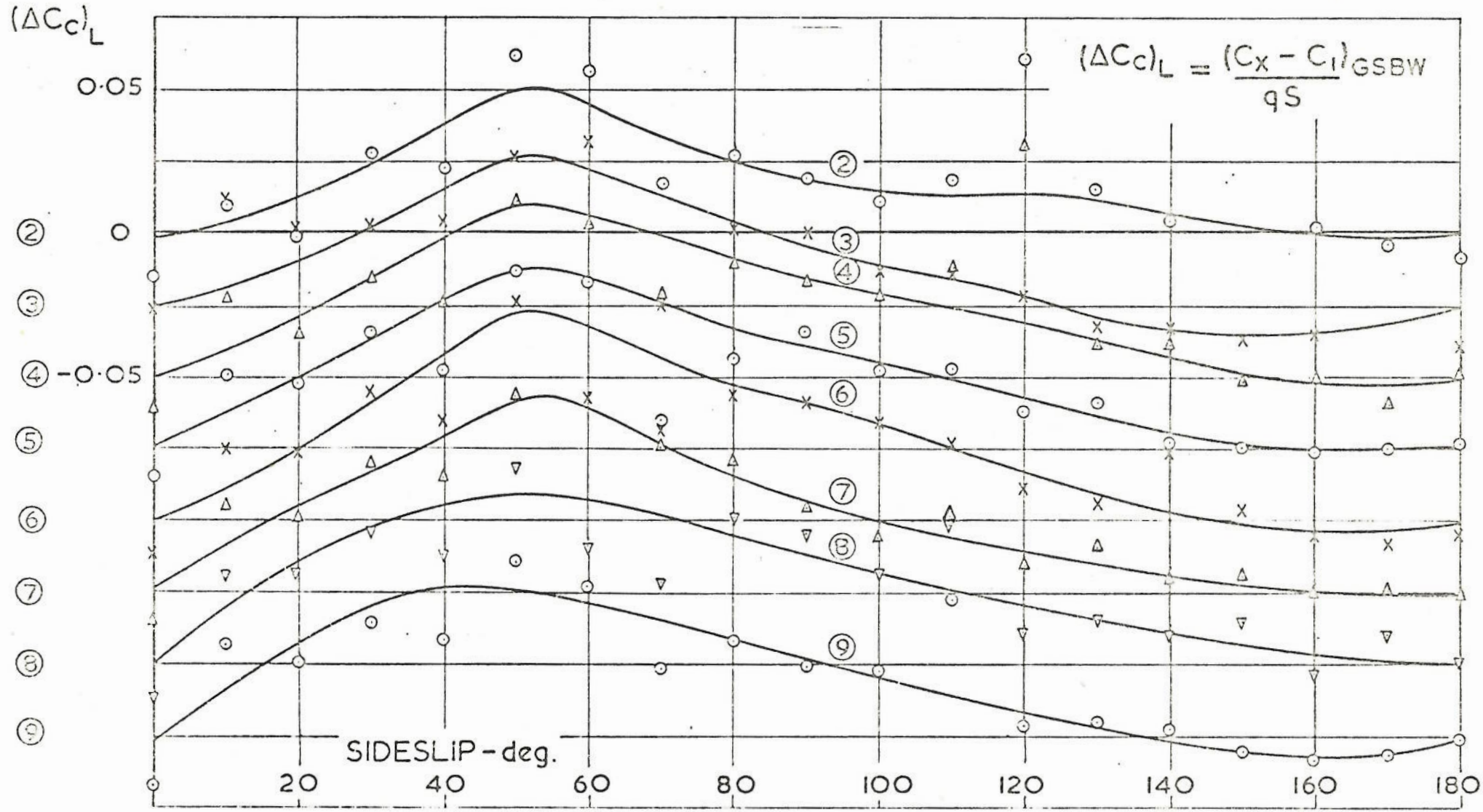

FIG. 20. INCREMENT OF CROSSWIND FORCE DUE TO PORT LOCATION.
$C_{Q1} = 0·0365$

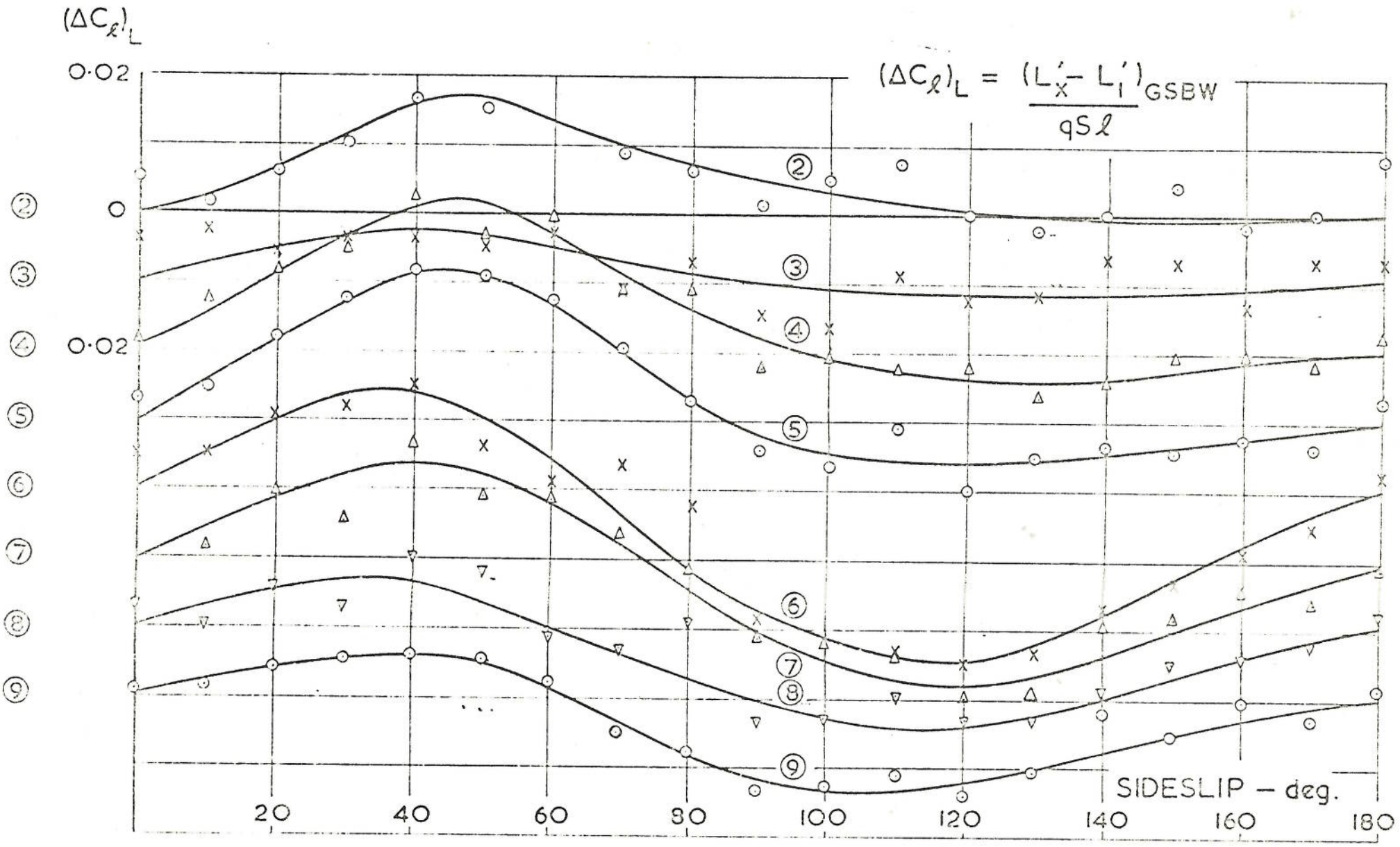

FIG. 21. INCREMENT OF ROLLING MOMENT DUE TO PORT LOCATION.
$C_{Q_I} = 0·0365$

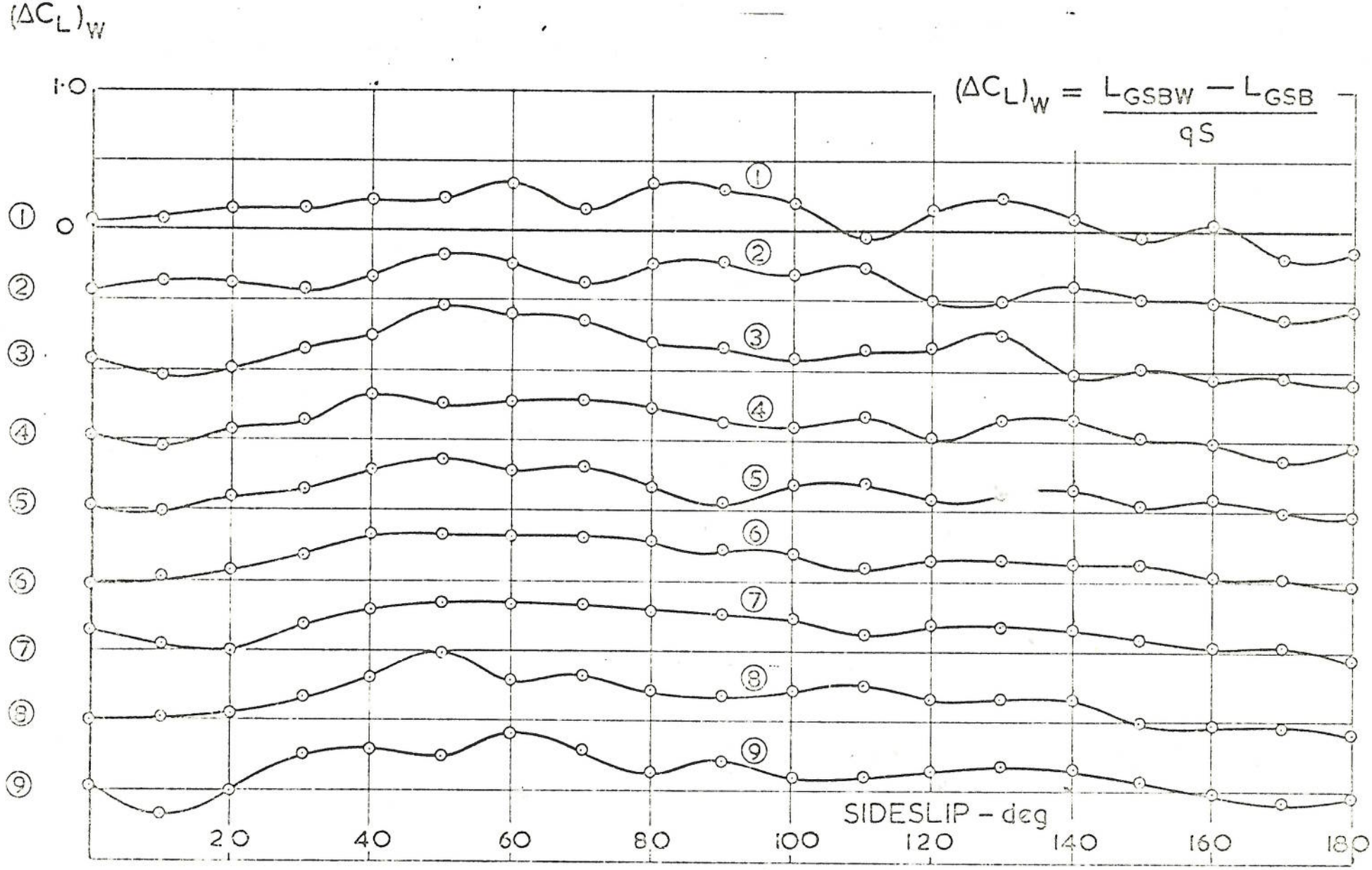

FIG. 22. LIFT INCREMENTS DUE TO WIND. $C_{Q_1} = 0{\cdot}0365$

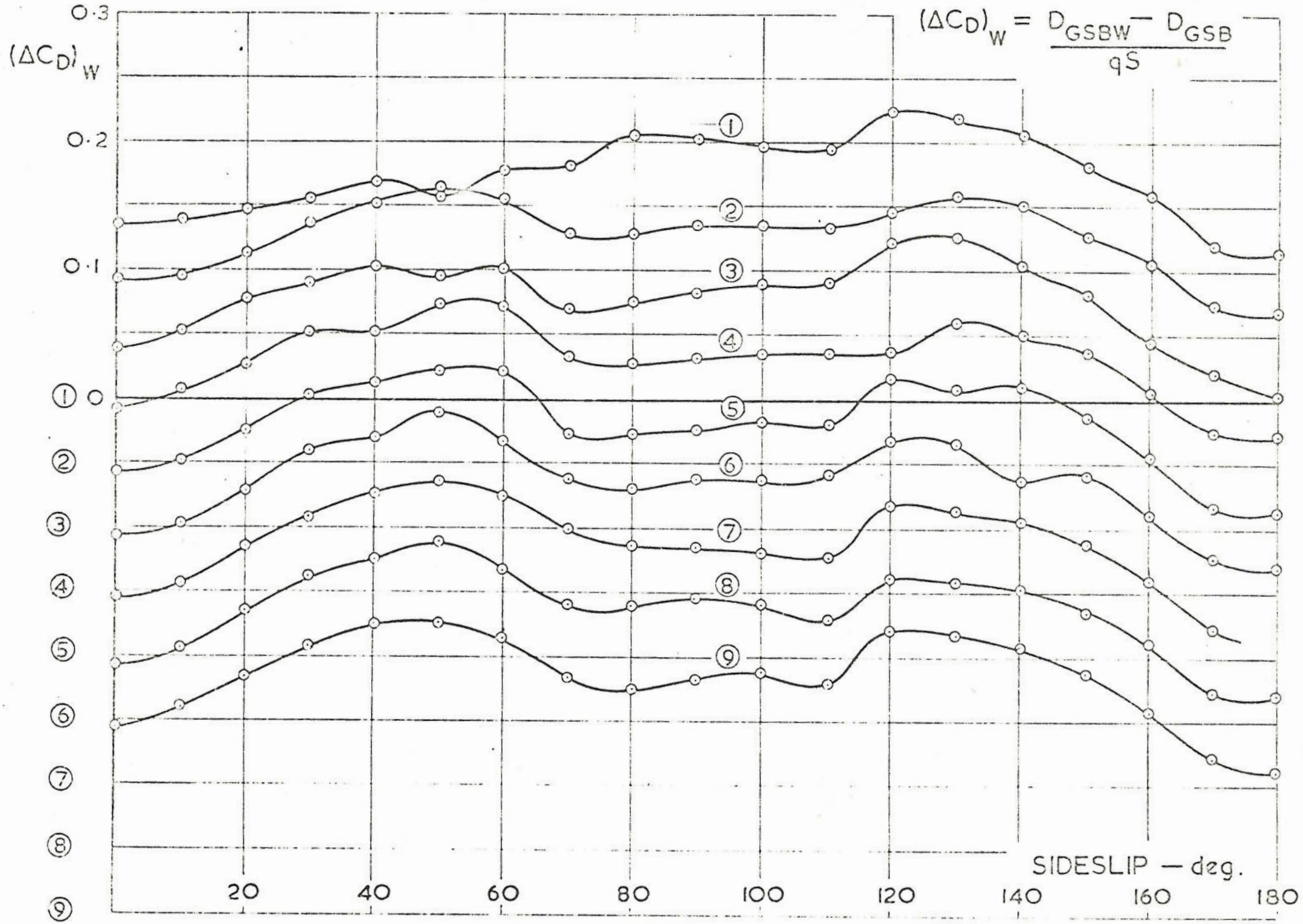

FIG. 23. DRAG INCREMENT DUE TO WIND. $C_{Q_1} = 0{\cdot}0365$

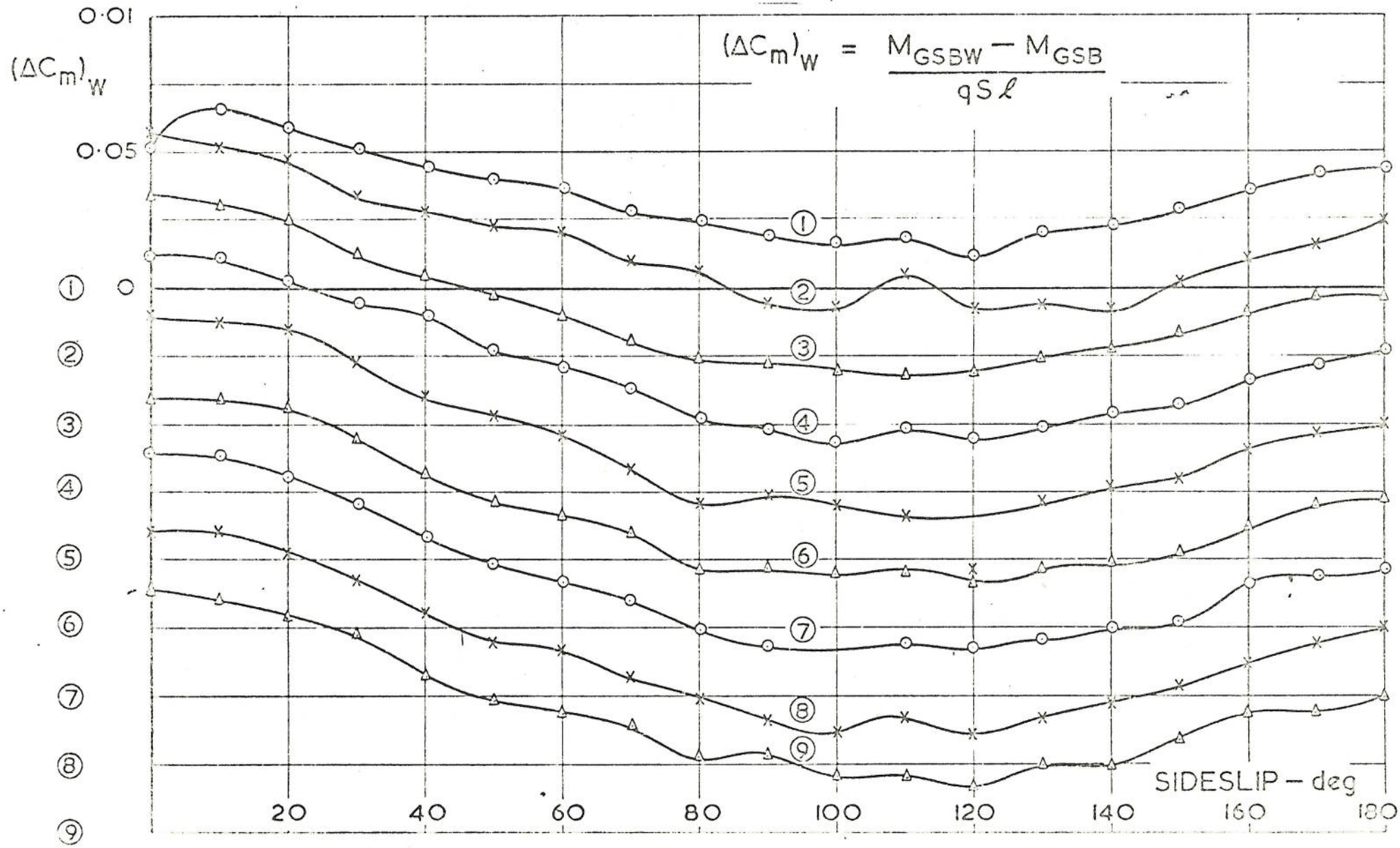

FIG. 24. PITCHING MOMENT INCREMENT DUE TO WIND. $C_{Q_1} = 0{\cdot}0365$

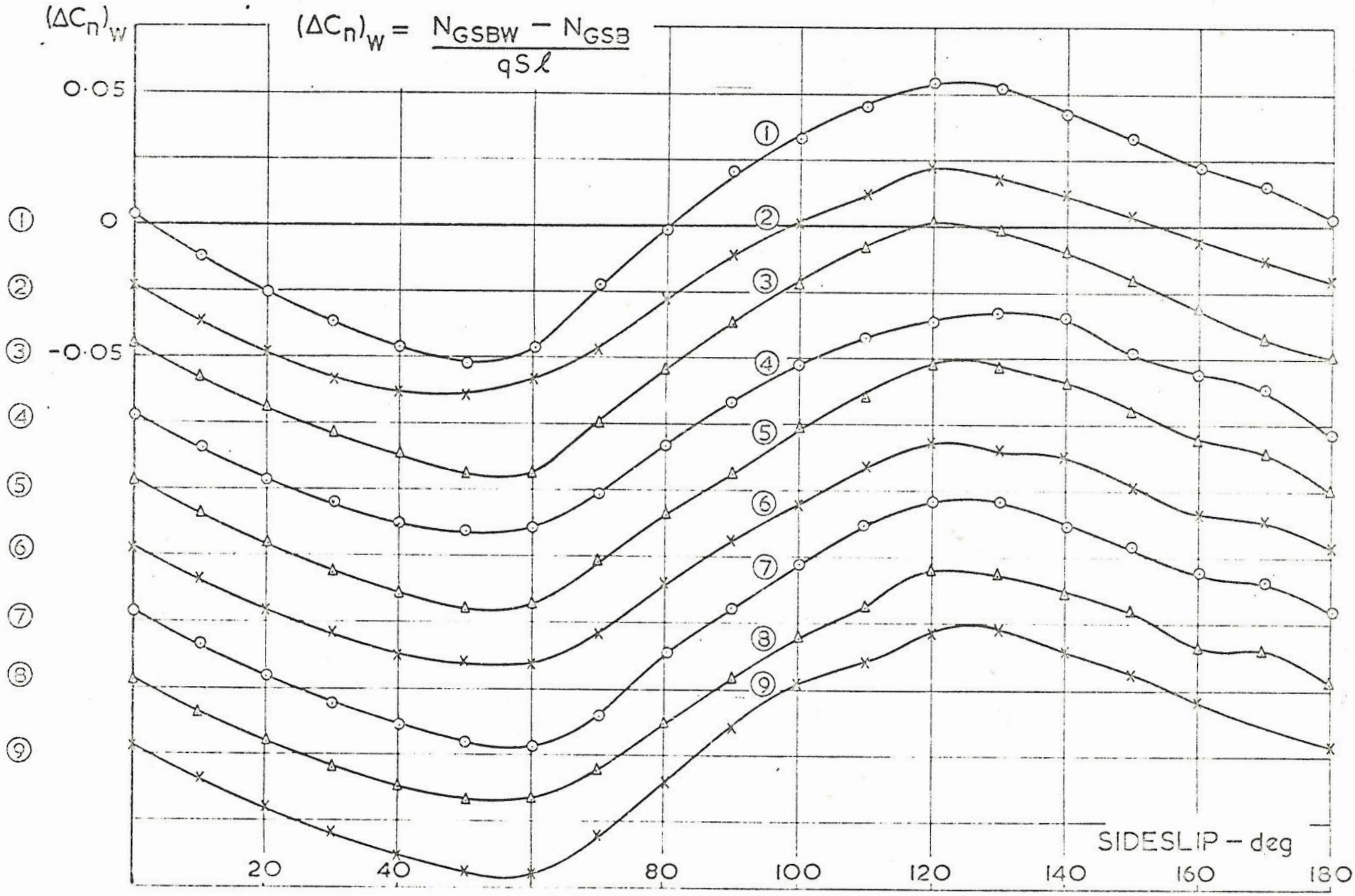

FIG.25. YAWING MOMENT INCREMENT DUE TO WIND. $C_{q_1} = 0{\cdot}0365$

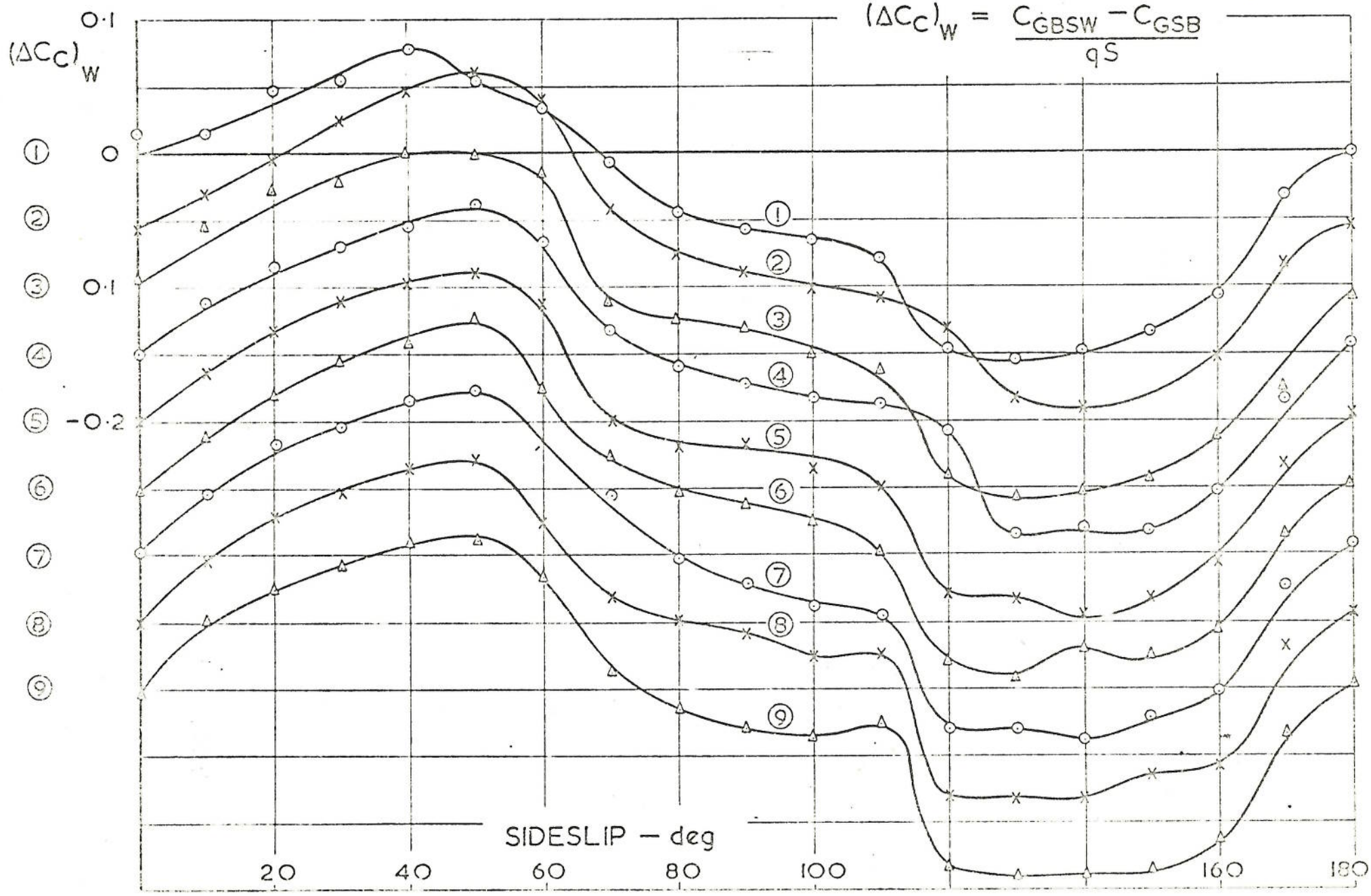

FIG. 26. CROSSWIND FORCE INCREMENT DUE TO WIND. $C_{Q_1} = 0{\cdot}0365$

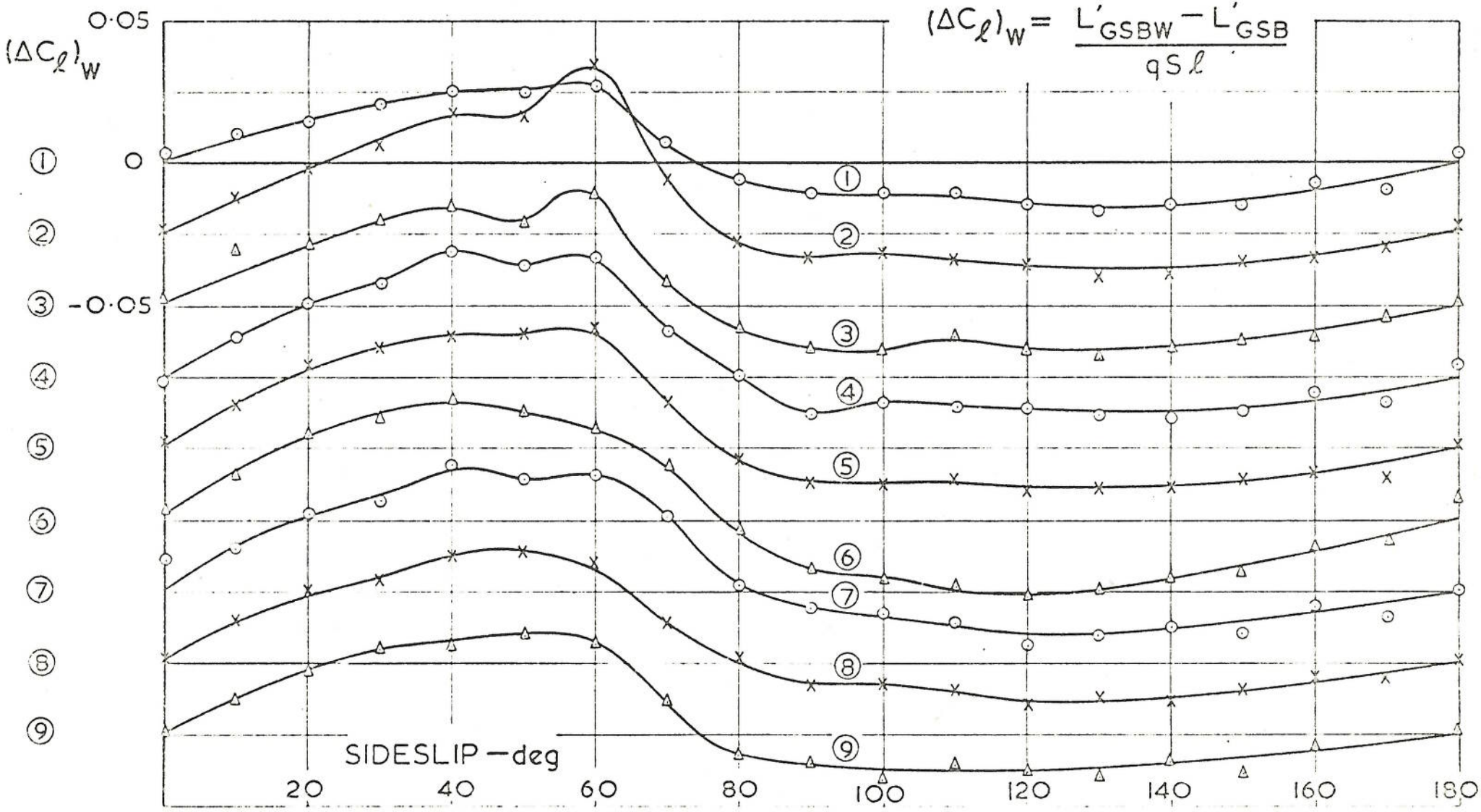

FIG. 27. ROLLING MOMENT INCREMENT DUE TO WIND. $C_{Q_1} = 0{\cdot}0365$

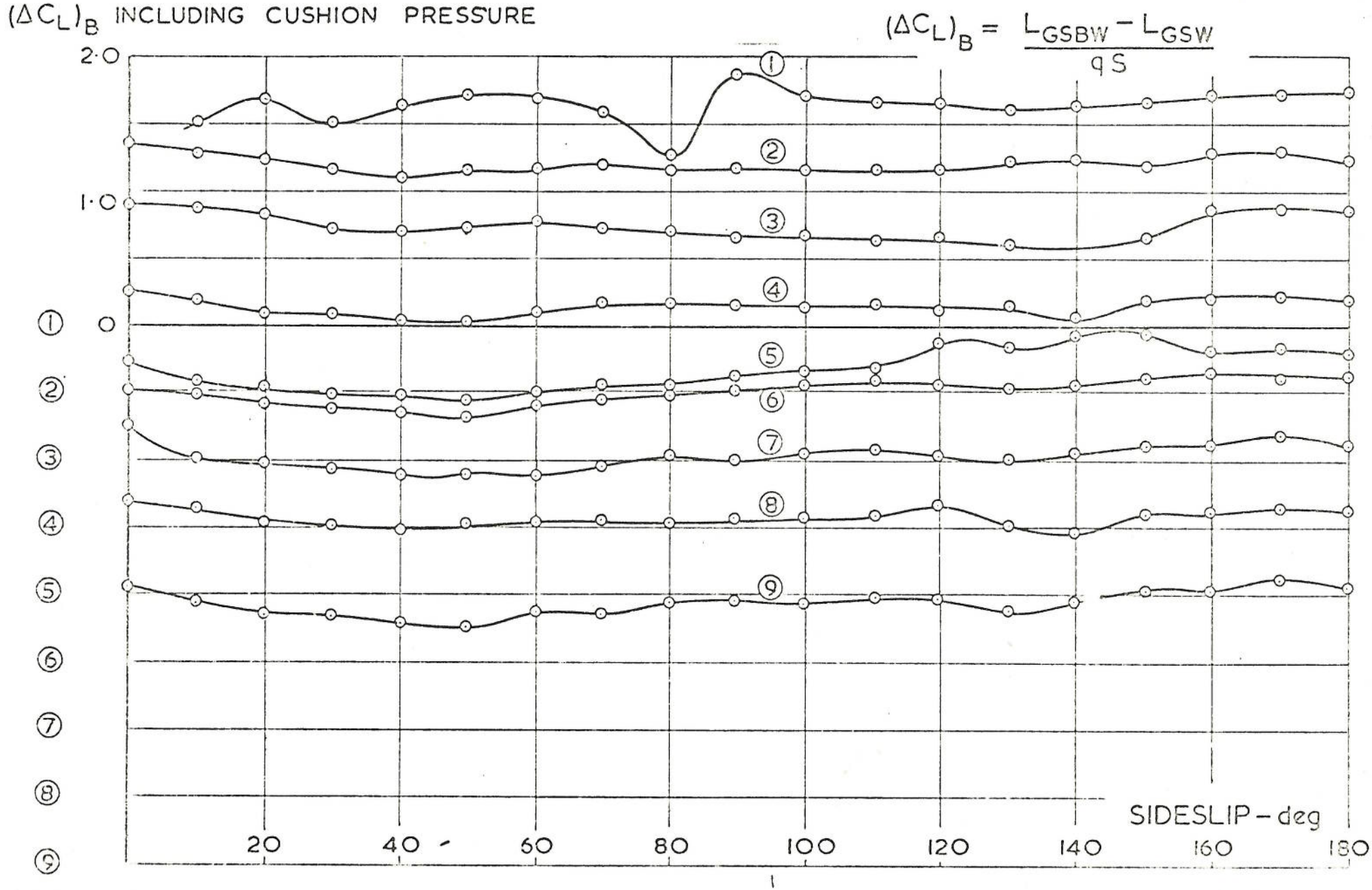

FIG. 28. LIFT INCREMENTS DUE TO BLOWING. $C_{Q_1} = 0{\cdot}0365$

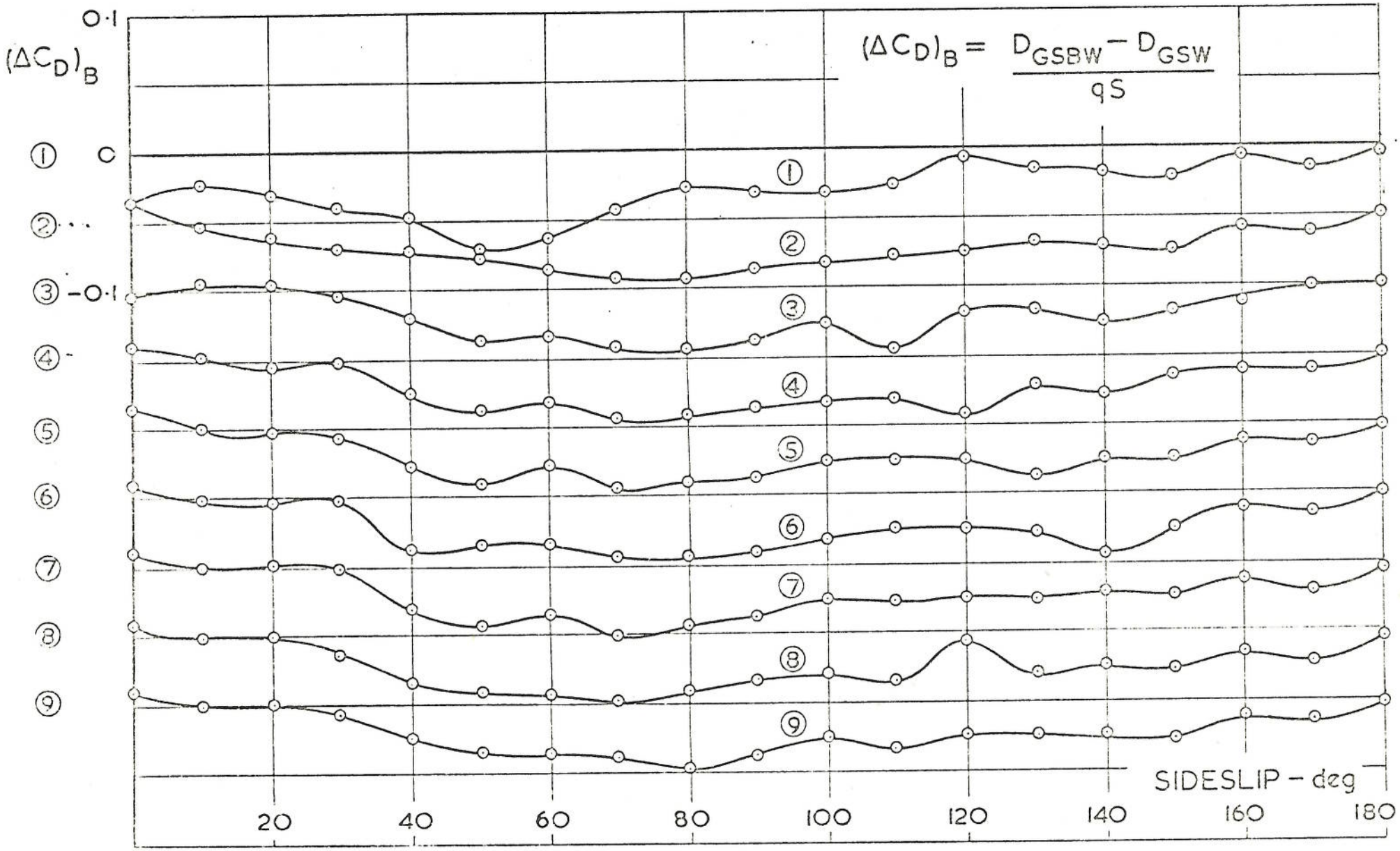

FIG. 29 DRAG INCREMENT DUE TO BLOWING, $C_Q = 0{\cdot}0365$

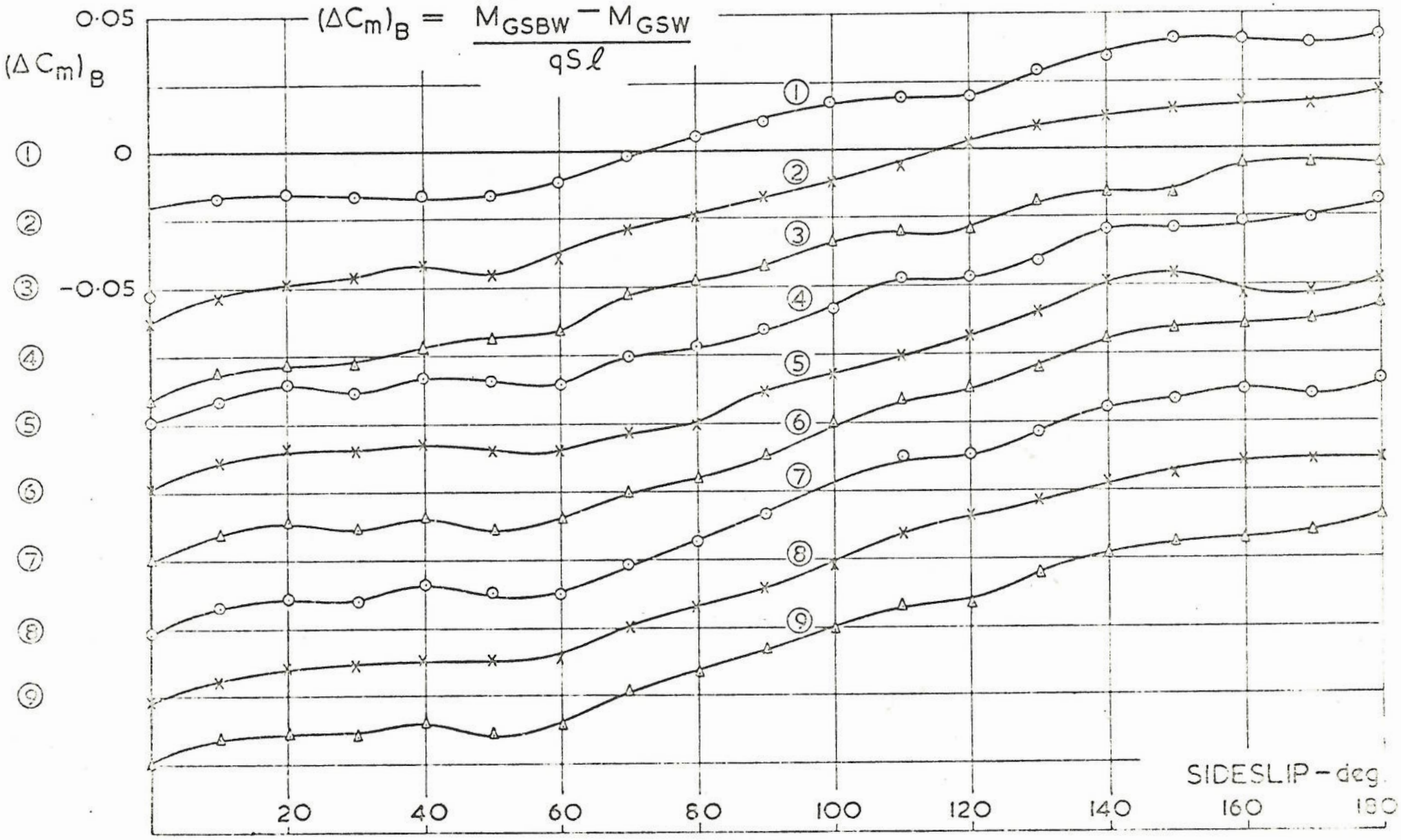

FIG. 30. PITCHING MOMENT INCREMENTS DUE TO BLOWING. $C_Q = 0{\cdot}036$

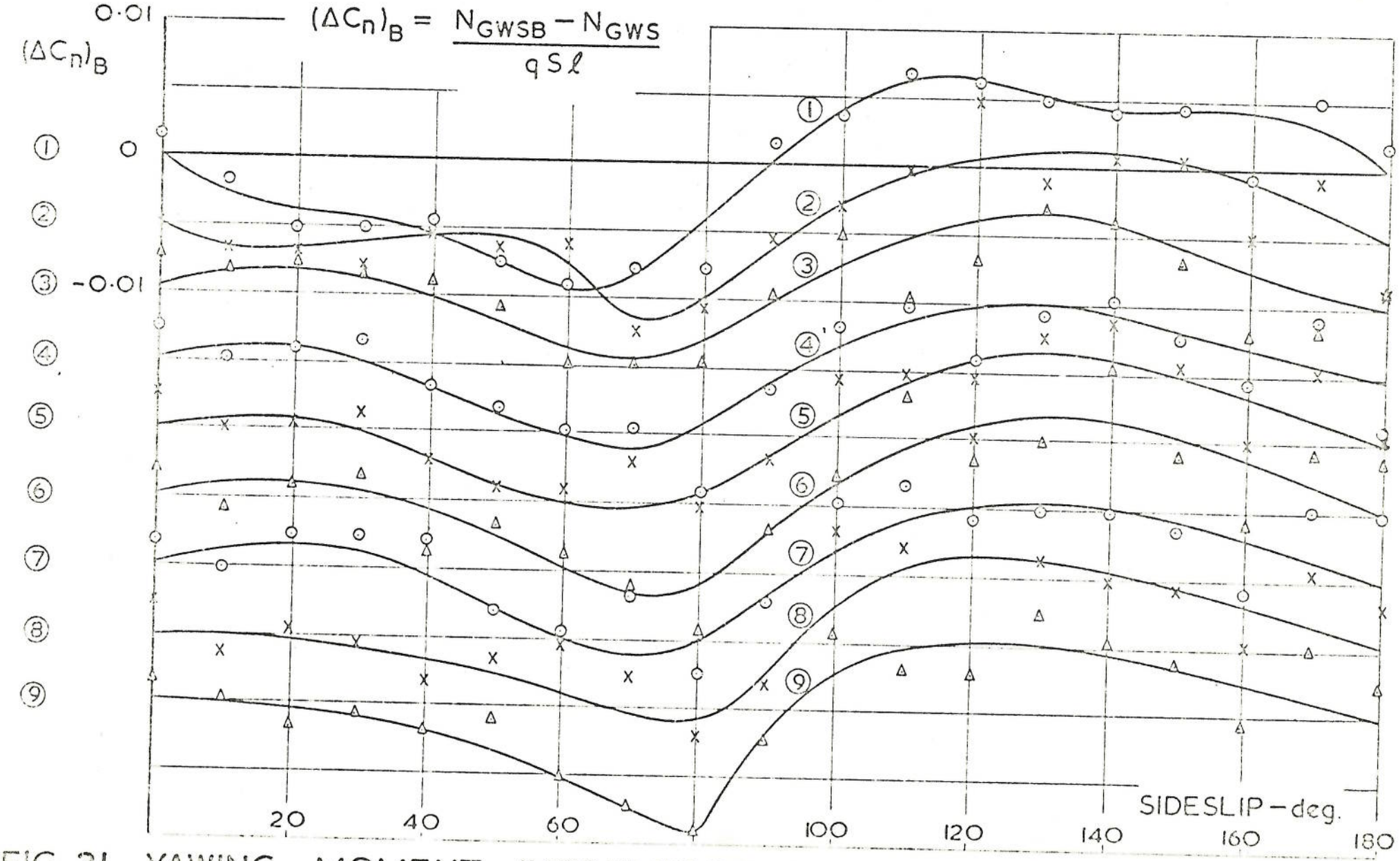

FIG. 31. YAWING MOMENT INCREMENTS DUE TO BLOWING. $C_{Q_1} = 0{\cdot}0365$.

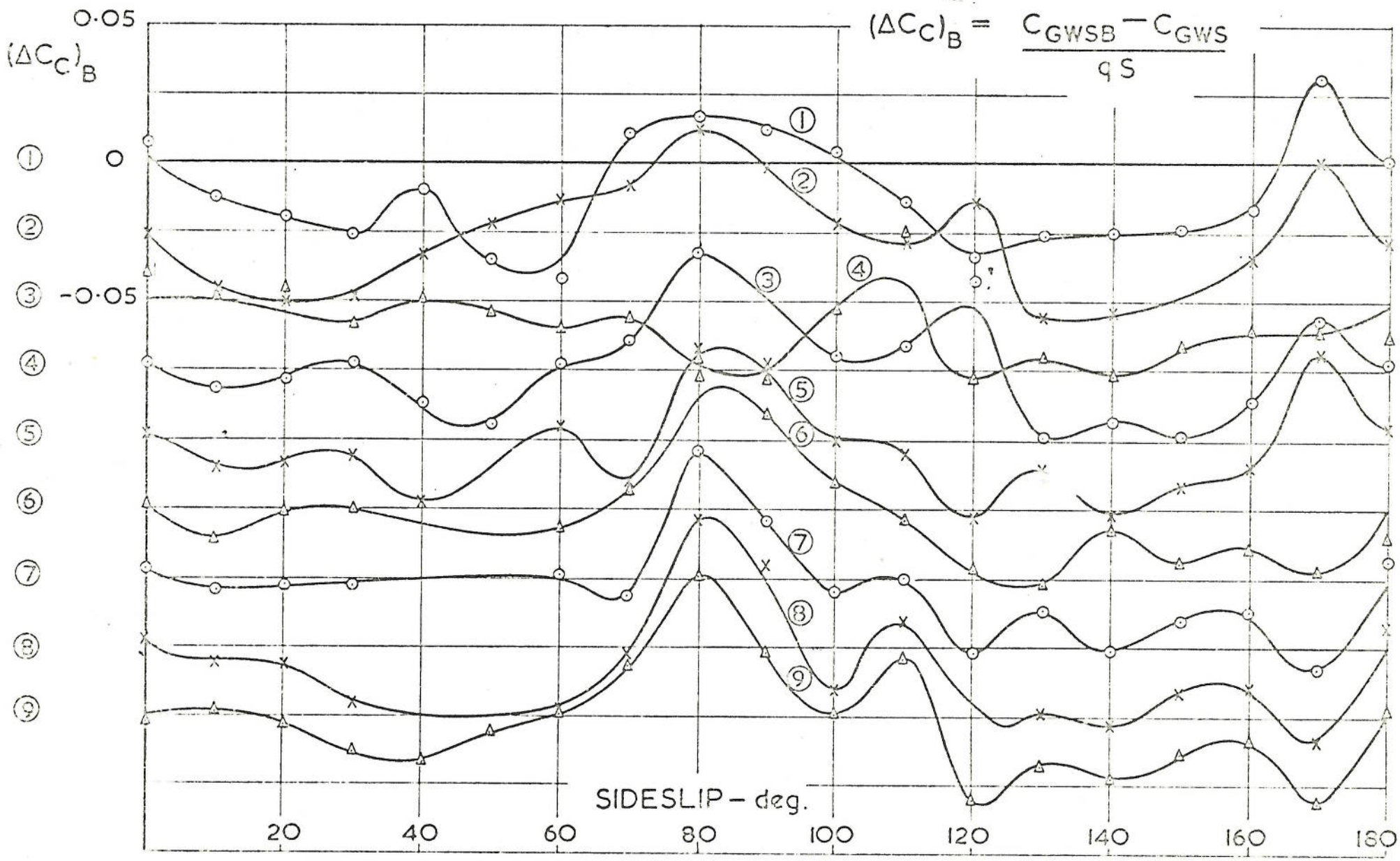

FIG. 32. CROSSWIND FORCE INCREMENTS DUE TO BLOWING. $C_{Q_1} = 0{\cdot}0365$.

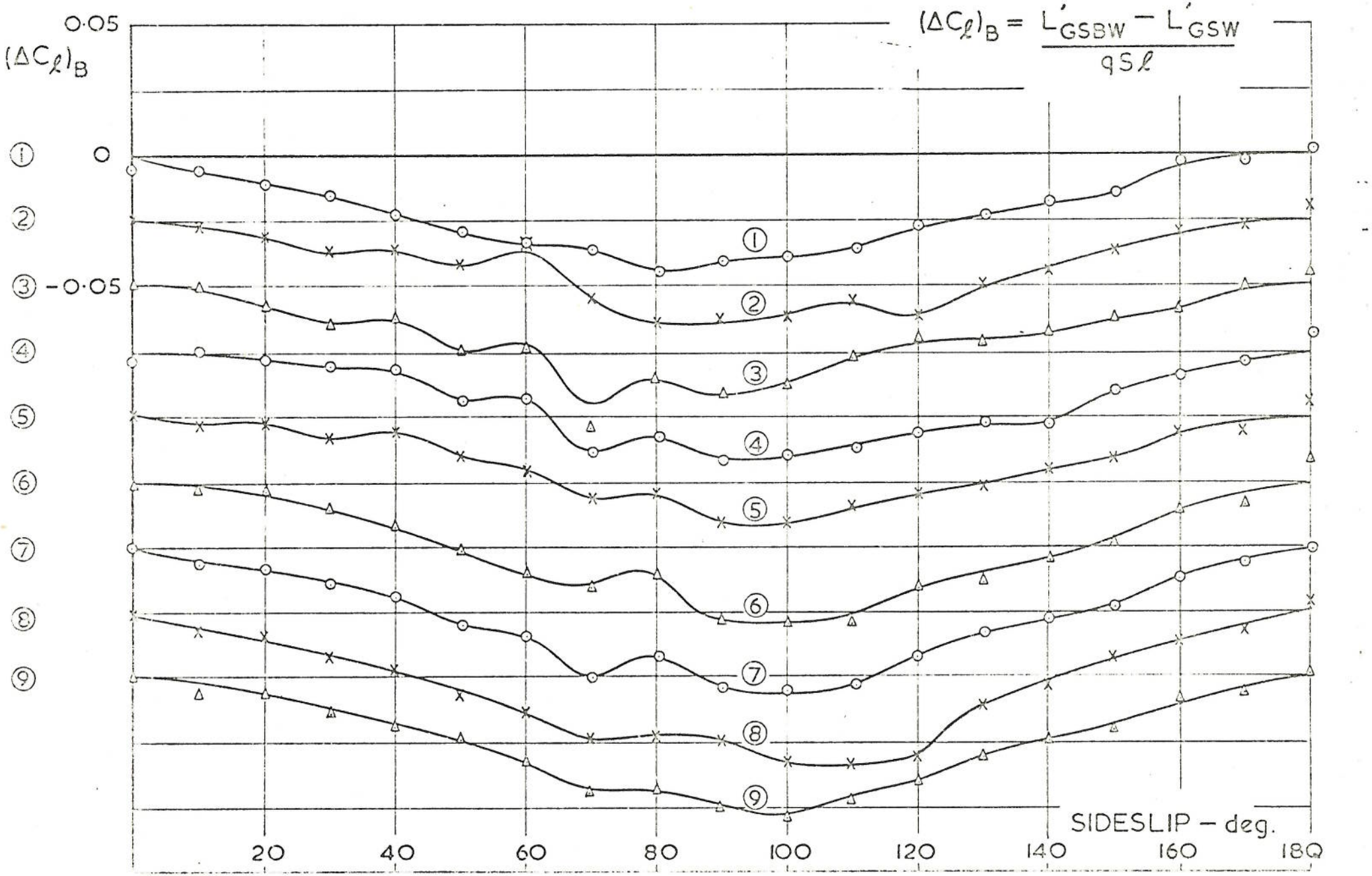

FIG. 33. ROLLING MOMENT INCREMENTS DUE TO BLOWING. $C_{Q_1} = 0{\cdot}0365$.

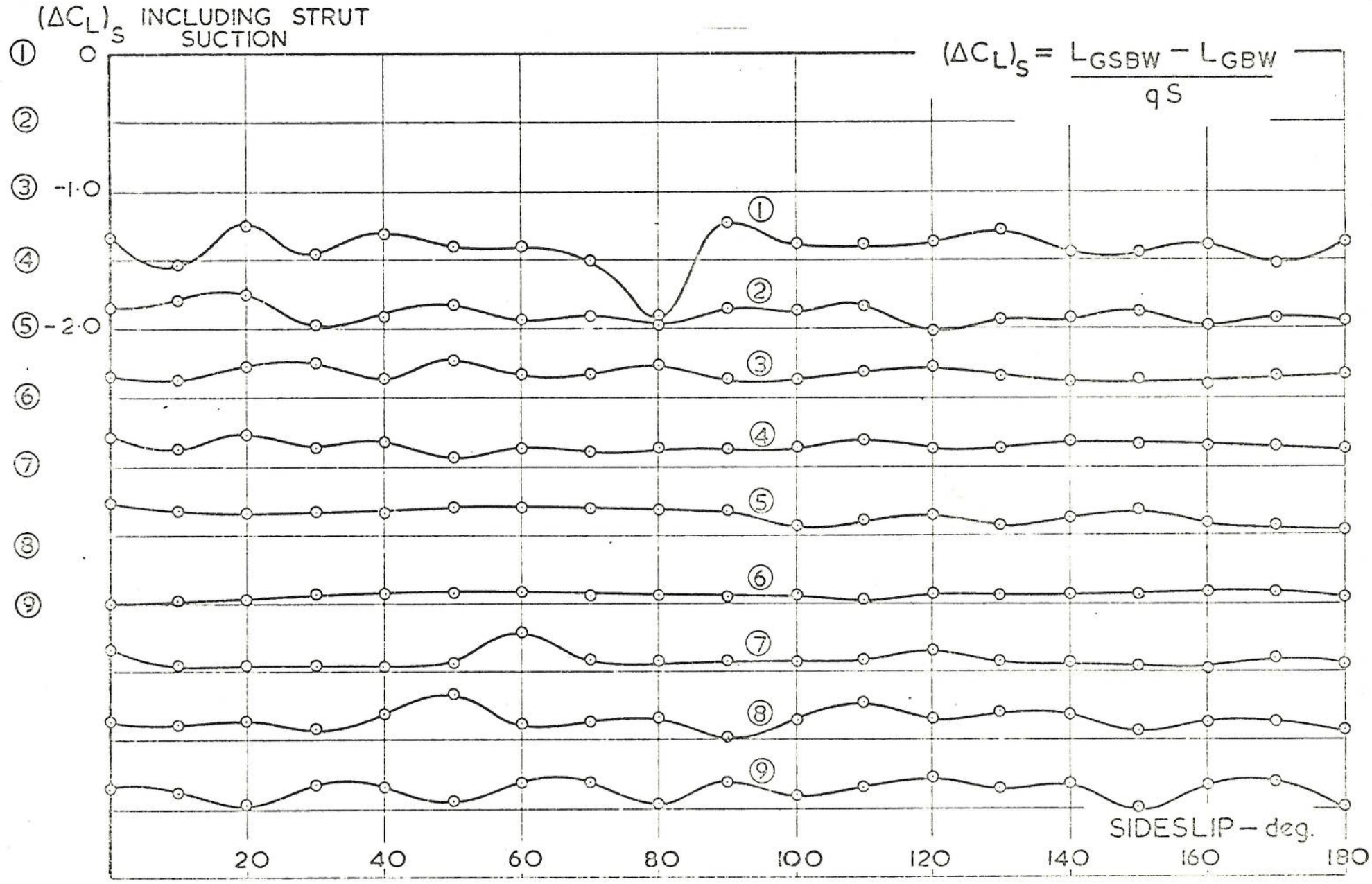

FIG. 34. LIFT INCREMENTS DUE TO SUCTION. $C_{Q_1} = 0{\cdot}0365$.

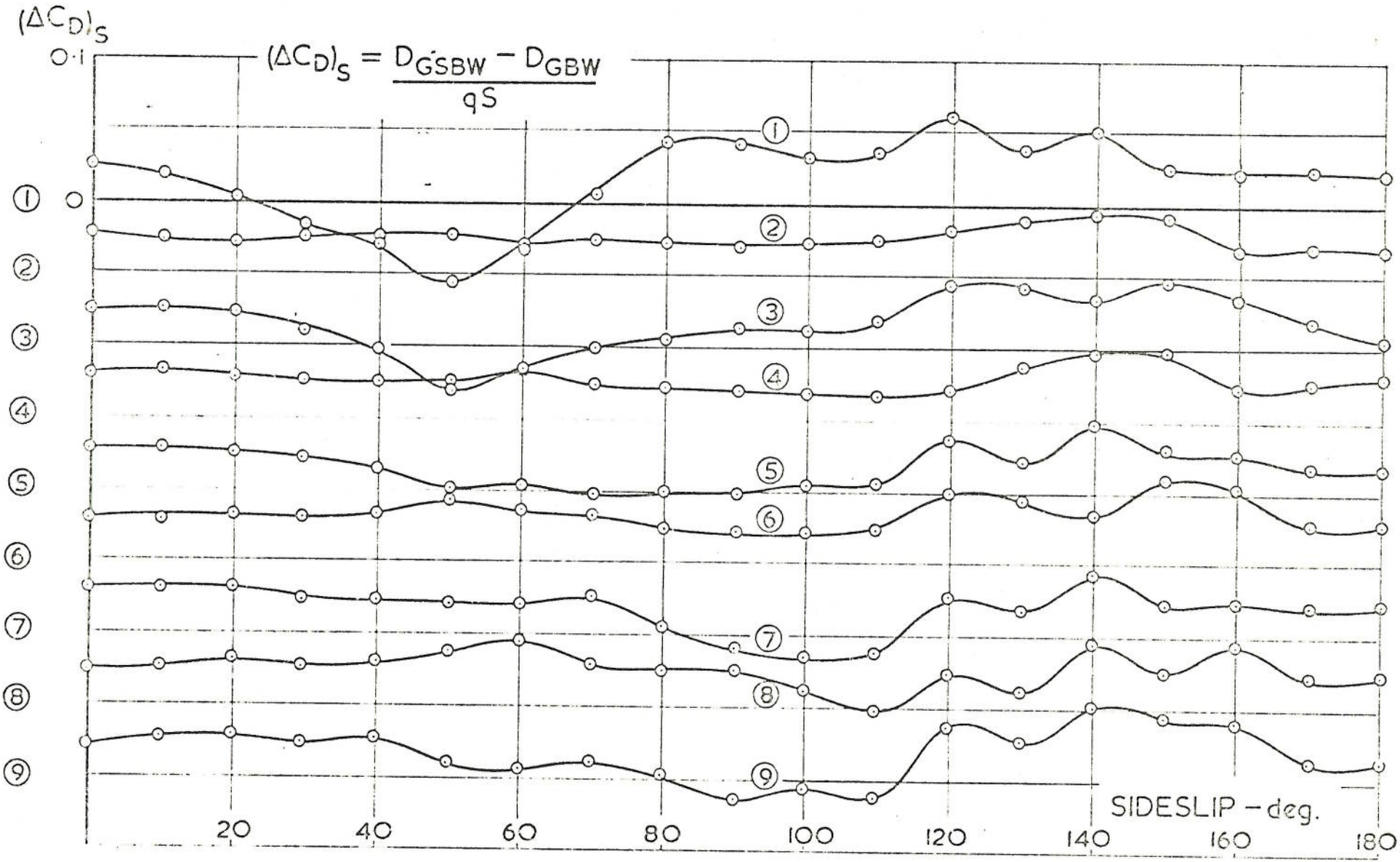

FIG. 35. DRAG INCREMENTS DUE TO SUCTION. $C_{Q_1} = 0{\cdot}0365$.

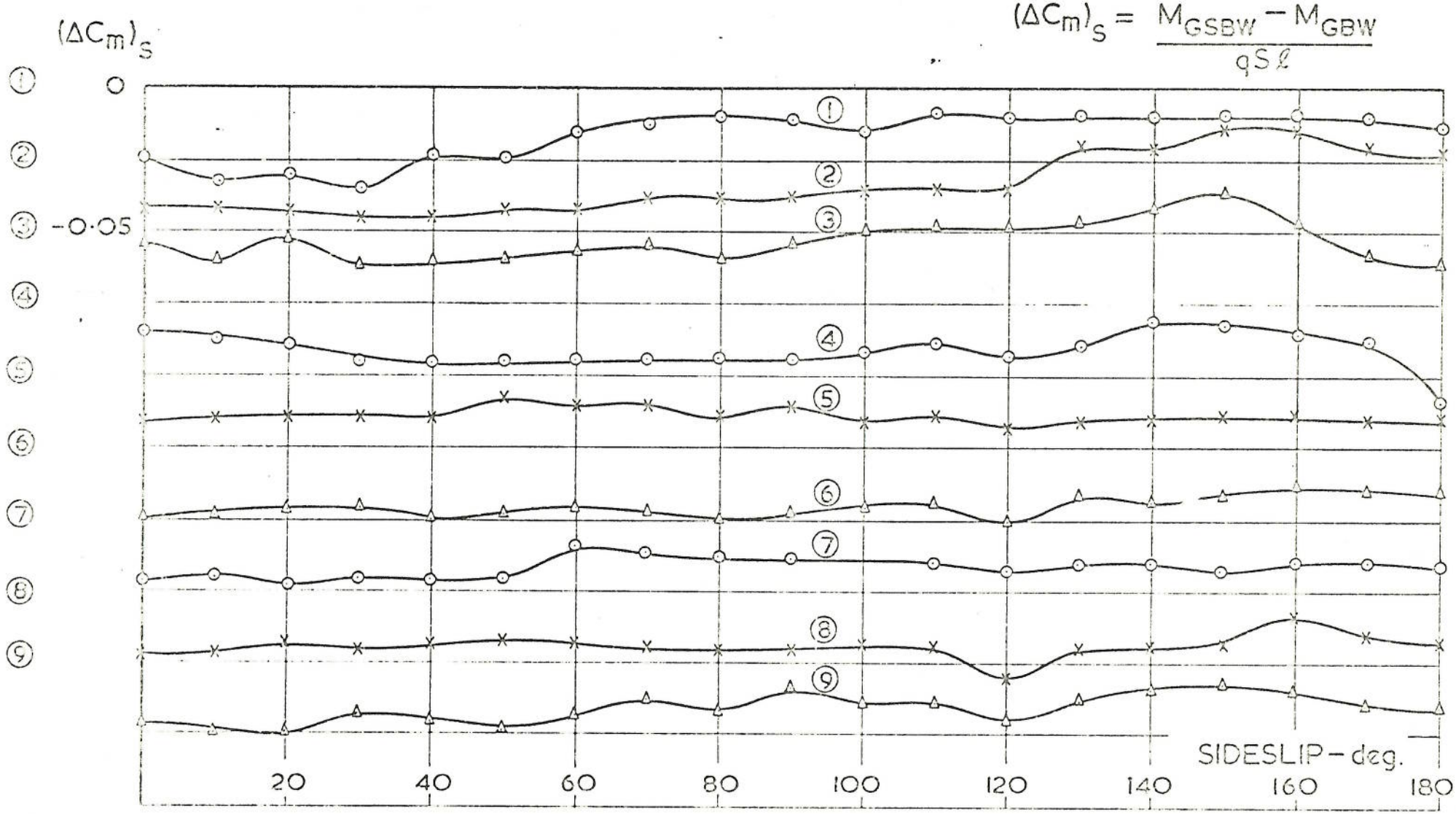

FIG. 36. PITCHING MOMENT INCREMENTS DUE TO SUCTION. $C_{Q_1} = 0{\cdot}0365$

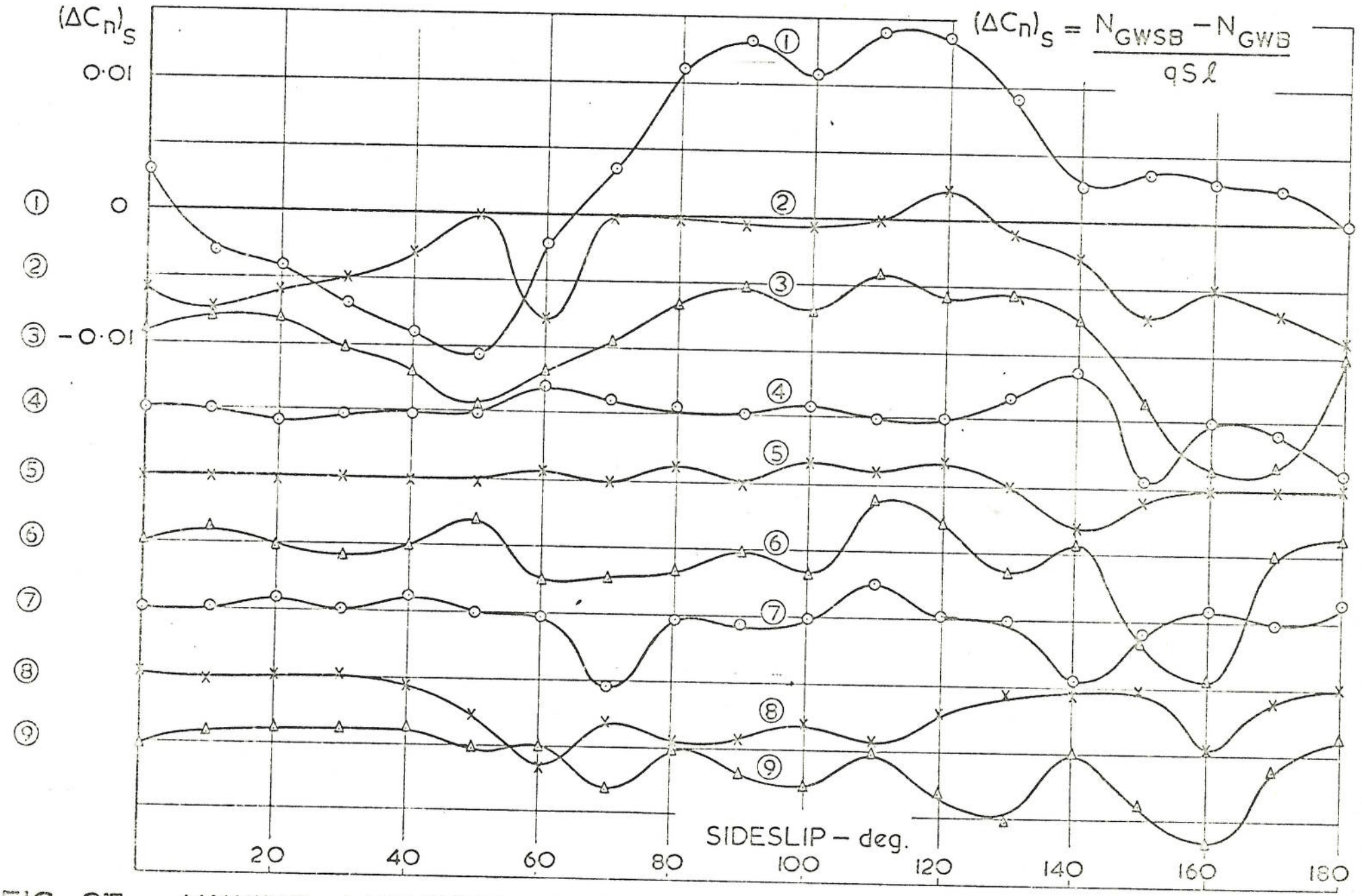

FIG. 37. YAWING MOMENT INCREMENTS DUE TO SUCTION. $C_{Q_1} = 0{\cdot}0365$.

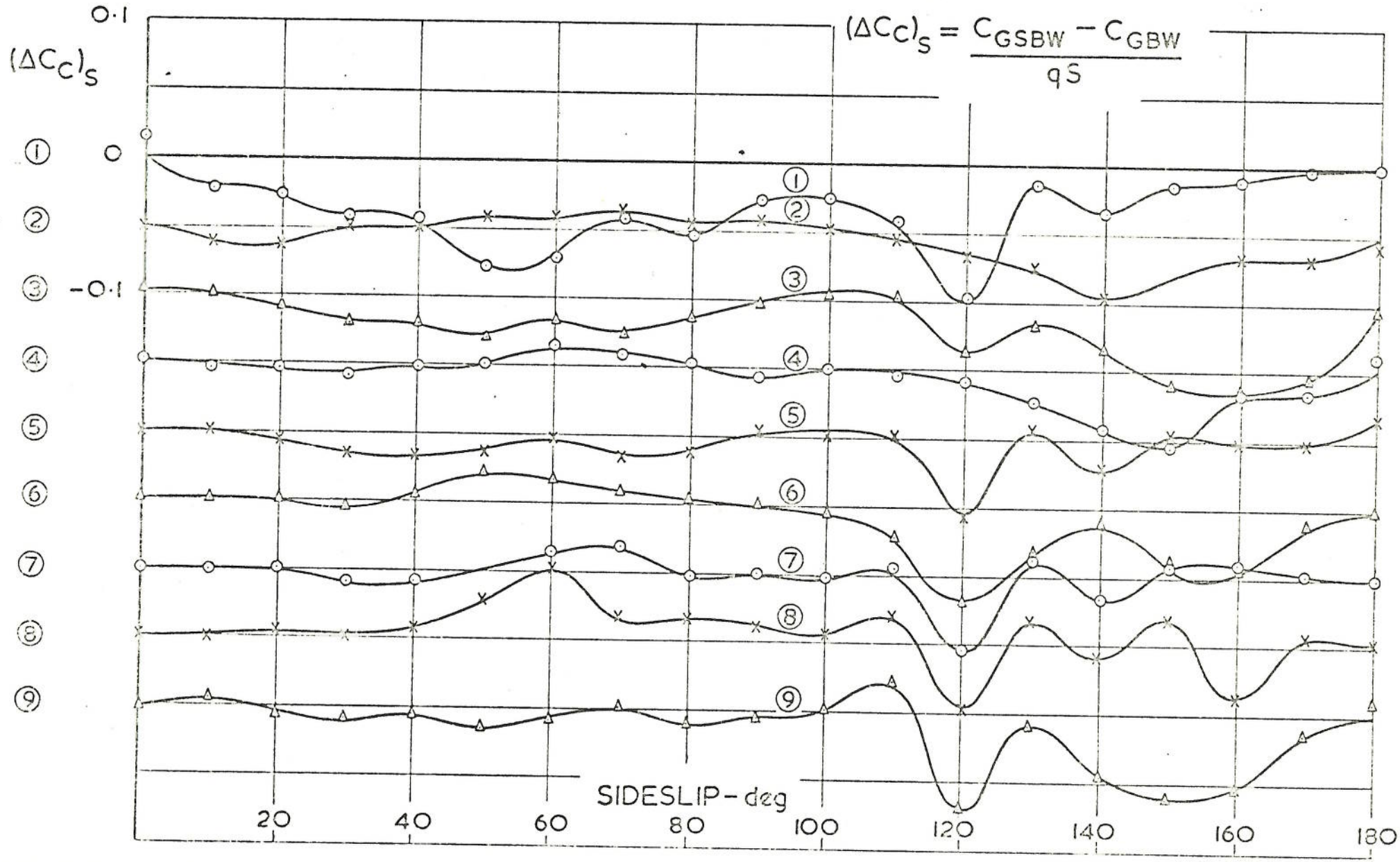

FIG. 38. CROSSWIND FORCE INCREMENTS DUE TO SUCTION. $C_{q_1} = 0{\cdot}0365$

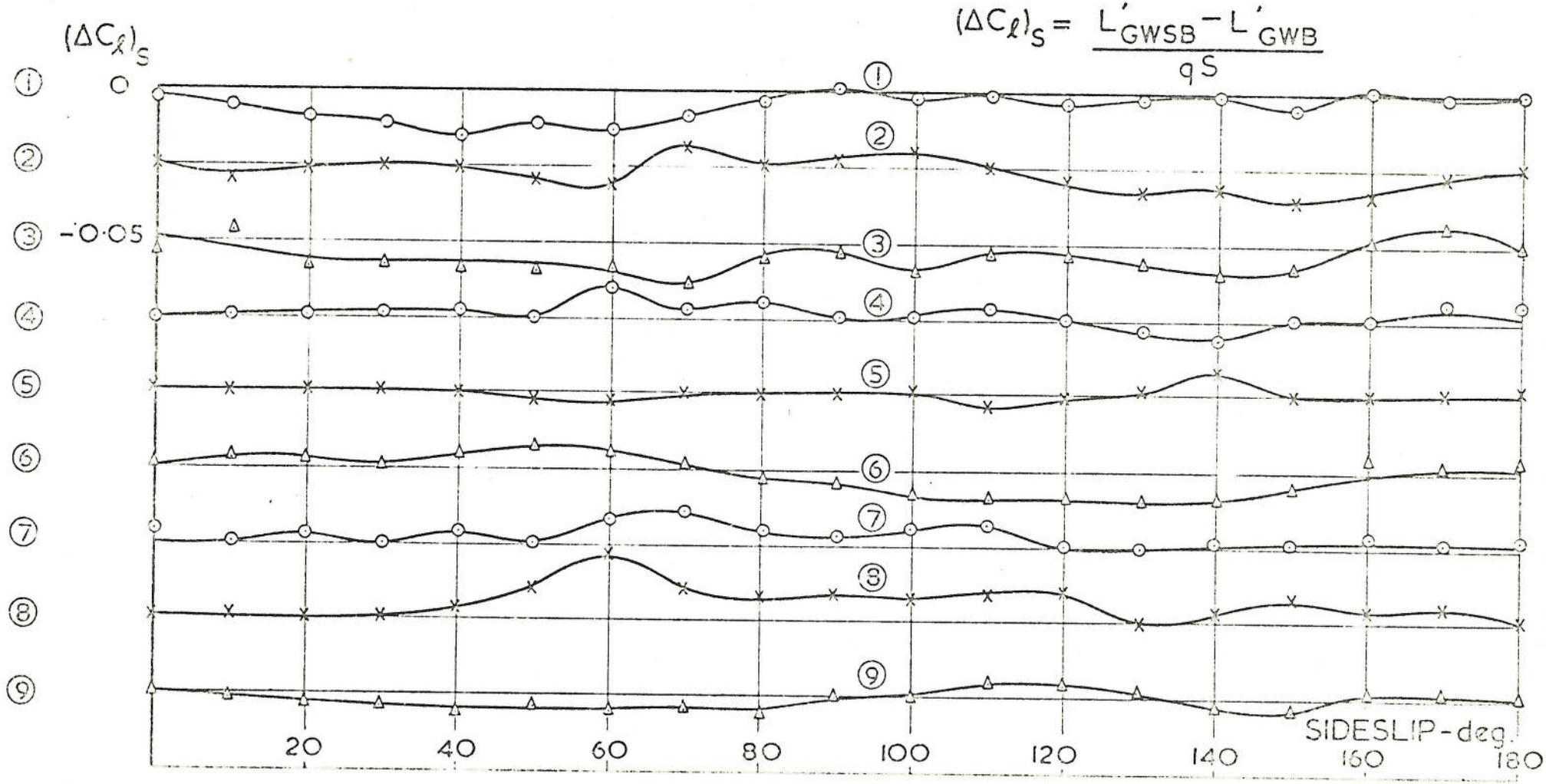

FIG. 39. ROLLING MOMENT INCREMENTS DUE TO SUCTION. $C_{Q_1} = 0{\cdot}0365$.

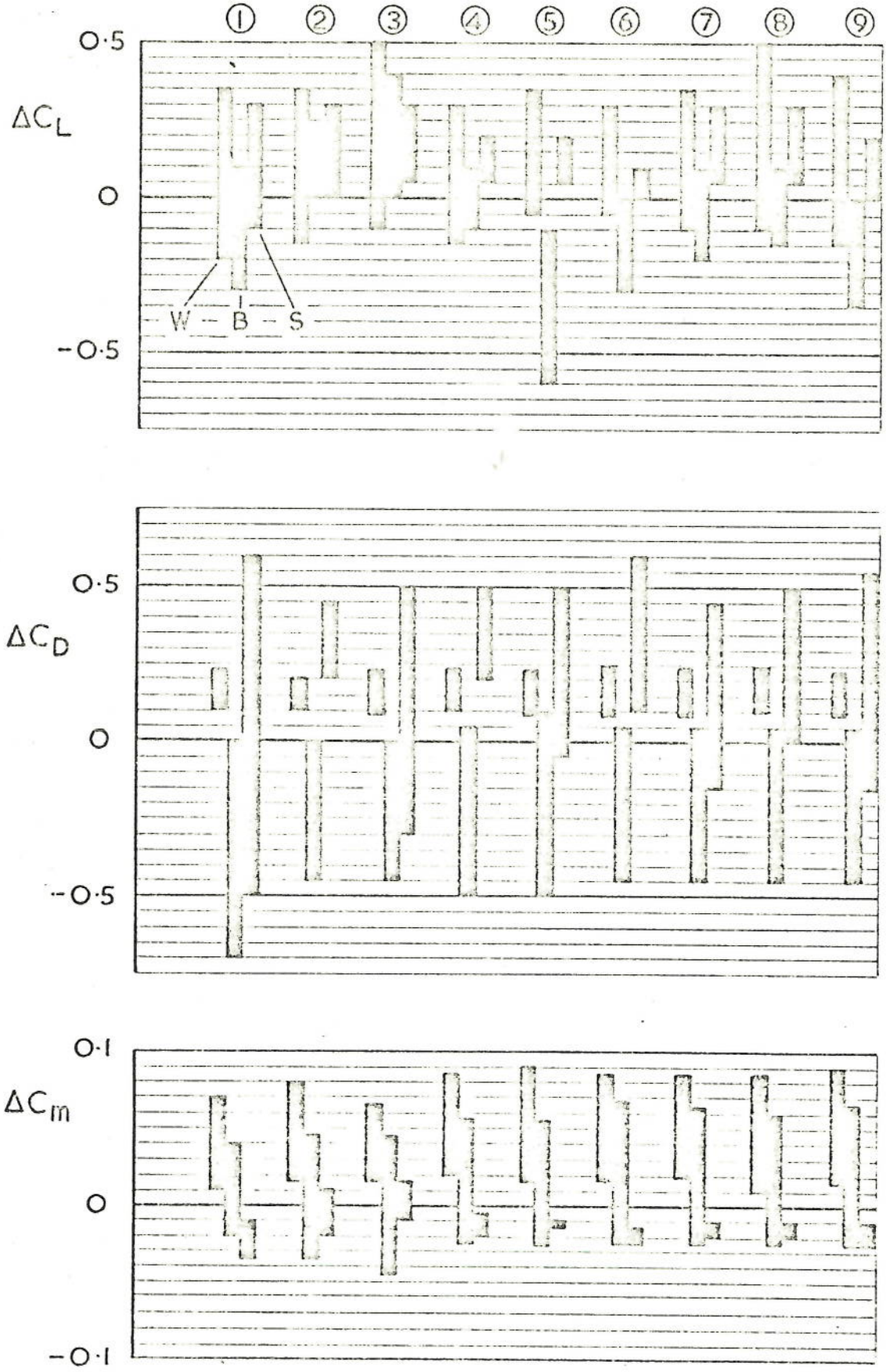

FIG. 40. INDIVIDUAL EFFECTS DUE TO WIND, BLOWING AND SUCTION.
$C_{Q_1} = 0 \cdot 0365$

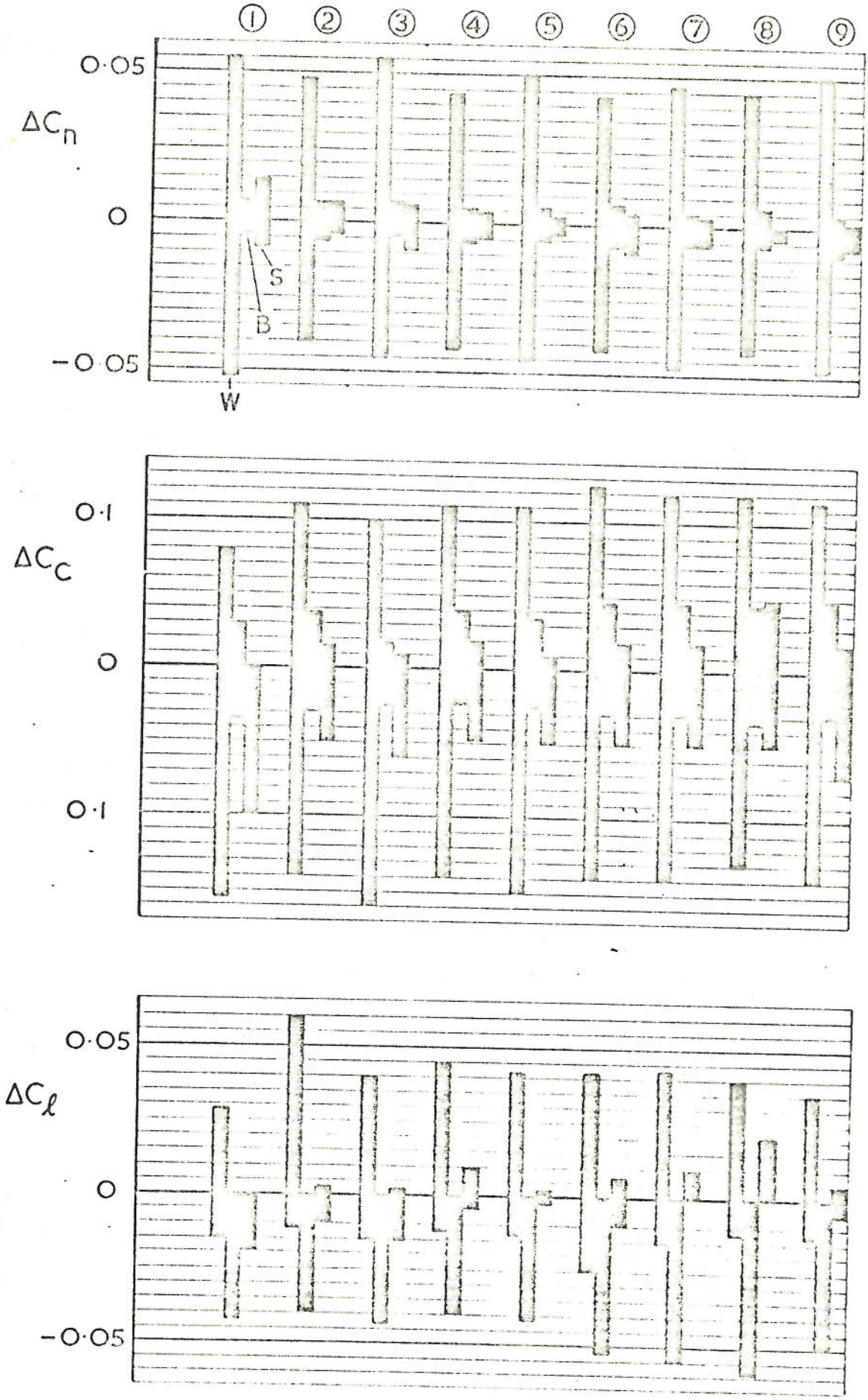

FIG. 41. INDIVIDUAL EFFECTS DUE TO WIND, BLOWING AND SUCTION.
$C_{Q_1} = 0{\cdot}0365$

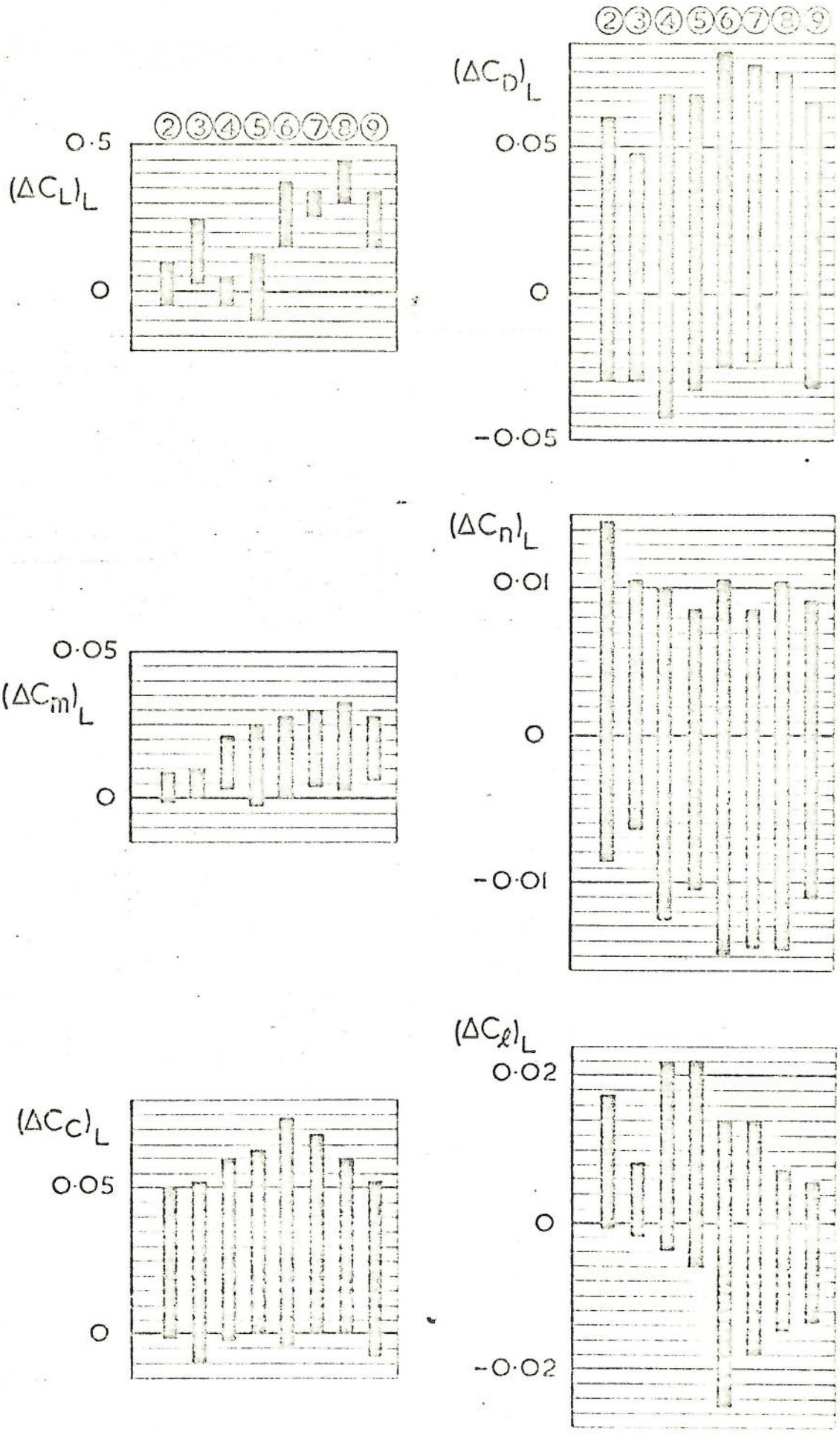

FIG. 42. EFFECTS OF PORT LOCATION.
$C_{Q_i} = 0·0365$